HIRDLS

HIGH RESOLUTION DYNAMICS LIMB SOUNDER

Originators: Ravi Gondhalekar

Date: September 17,1999.

Subject / Title: **HIRDLS PCU Finite Element Analysis**

Contents / Description / Summary:

This Document describes the finite element stress and normal mode analysis performed on the HIRDLS PCU (Power Converter Unit). The analysis shows that the mechanical assembly of the PCU is capable of carrying the maximum structural loads expected during launch within acceptable elastic deformation boundaries. It also shows that all natural frequencies of the mechanical assembly are above the set minimum not to cause resonance of the HIRDLS main structure.

Key Words: PCU Structural Analysis

Purpose (20 characters maximum):

Approved By: Nigel Morris

Date: September 17, 1999.

Rutherford Appleton Laboratory
Chilton, Didcot
Oxfordshire
OX11 0QX, United Kingdom

EOS

Table of Content

1. Summary

This Document describes the finite element stress and normal mode analysis performed on the HIRDLS PCU (High Resolution Dynamic Limb Sounder Power Converter Unit). The analysis shows that the mechanical assembly of the PCU is capable of carrying the maximum structural loads expected during launch within acceptable elastic deformation boundaries. It also shows that all natural frequencies of the mechanical assembly are above the set minimum not to cause resonance of the HIRDLS main structure.

2. Introduction

During launch a spacecraft is subjected to violent accelerations; linear acceleration in the direction of flight and oscillating accelerations in every direction due to vibration of the vehicle.

An analysis was needed in order to predict the mechanical behavior of the PCU. There are two motivations for this:

1. To verify that the system hardware is structurally sound. Deflection is unavoidable but must be kept as small as possible and to well within the material's elastic limit to avoid plastic deformation and possible fracture.

2. To confirm there is no natural frequency that could interfere with the main structure of HIRDLS and cause resonant conditions. The lower limit for a first natural frequency is set at 100Hz. All components' natural frequencies must exceed this.

The analysis was performed using finite element methods within SDRC I-DEAS (Structural Dynamics Research Corporation Integrated Design Engineering Analysis Software). This report will cover the creation of the finite element model, an examination of the results and a discussion on the accuracy and validity of the model. Appendix I contains images of the HIRDLS PCU.

3. Applicable Documents

Document: SP-HIR-036: Power Converter Unit Subsystem Specification Document.
Document: SP-HIR-218: Power Converter Unit Interface Control Document.

4. The Model

4.1 Finite Element Models under I-DEAS

I-DEAS is a 3-Dimensional modeling package. It allows the user to create 3D parts that can be used for finite element analysis. Before a finite element analysis can be performed the part must be broken up into a number of finite elements. This is called meshing and the resultant collection of elements is the mesh. A node is created on the corner of each of these elements. There are two ways a finite element mesh can be created.

1. A part can be modeled and then automatically meshed by the software. The mesh will be produced to a quality pre-defined by the user (element type, size, minimum angles, etc.). This is the quickest way of producing a mesh however the user has little control over the exact position of the elements as they are created at random.

2. The mesh can be created manually. This is a more tedious method of mesh generation but gives extra control over mesh geometry as the user individually constructs the elements.

4.2 Construction of the PCU Model

The large components of hardware like side panels were modeled as parts then automatically meshed. Finer details and electronic components were added later manually. Appendix II contains images of the HIRDLS PCU finite element mesh.

A number of different types of elements were used in the model; Thin Shell (quadrilateral and triangular), Rigid Bar, Linear Beam and Lumped Mass. Different types of elements are a tool to make the model more realistic and easier to solve. Table 1 below summarizes the use of different elements.

Table 1.

Element Type	Number Off
Thin Shell (quadrilateral)	6035
Thin Shell (triangular)	914
Rigid Bar	273
Linear Beam	87
Lumped Mass	79

Total number of elements: 7388
Total number of nodes: 6745

4.3 Thin Shell Elements

The thickness of the panels is small compared to the length and width, so the stresses can be assumed constant throughout the thickness of the panels. The panels and circuit boards were not modeled as solids, rather as surfaces. By creating Thin Shell Elements a thickness is allocated to the elements. The panels will be modeled as solid, but the mesh will only be 2-Dimensional. The reason for doing this is to reduce processing requirements by removing unnecessary detail from the model. It is important to remember that the model does not have to look like the physical part but must behave in the same manner.

4.4 Rigid Bar Elements

A Rigid Bar Element is a massless, infinitely stiff connection between two nodes. There is no equivalent to this element in real life. In the PCU finite element model Rigid Bar Elements were used to simplify connections and mounting brackets that did not need to be explicitly modeled.

4.5 Linear Beam Elements

I-DEAS gives the option of creating Linear Beam Elements to model rod like parts. This simplifies the model by assuming a linear stress gradient along the length of the Linear Beam Element. This type of element was used to mount circuit boards within the PCU.

4.6 Lumped Masses

Lumped Masses can be introduced where the model has localized non-structural weight. This is a useful tool when modeling small but heavy components that do not contribute to the stiffness of the structure. Lumped Masses are used in the model to emulate components such as connectors, EMI-Filter and EMI-Converter-Modules.

4.7 Material Properties

Below are descriptions of the two materials employed by the model.

Aluminium Alloy BS1156082:

Youngs Modulus	$E = 69GPa$
Poissons Ratio	$\nu = 0.3$
Mass Density	$\rho = 2700kgm^{-3}$
0.2% Proof Stress	$\sigma_{y_{0.2\%}} = 270MPa$
Ultimate Tensile Stress	$\sigma_{UTS} = 310MPa$

Glass Fibre Reinforced Polymer (GFRP):

Youngs Modulus	$E = 15GPa$
Poissons Ratio	$\nu = 0.15$
Mass Density	$\rho = 1500kgm^{-3}$

The electronic circuit boards are made of GFRP. Everything else in the PCU model is constructed of Aluminium Alloy. In reality this is not the case. Many components are made of Steel, Copper or Delrin; screws, nuts, washers, earthing straps, mounts, leads etc.. None of these components are of structural importance, so have not been explicitly modeled.

This collection of almost negligible items has not been completely ignored however. They have been added in the form of a distributed mass. For every main component the collective weight of all minor parts attached to it has been added. Changing the mass density in the material specification for that component did this. The approximation has been made that the added weight of minor items is evenly distributed within the main component. For heavy items the density needed only slight manipulation, so the approximation is accurate.

This technique was also used to model circuit boards. The density of GFRP boards was inflated up to 500% to take into account electronic components. The accuracy of this example of density fixing is dubious, but proper modeling of circuit boards introduces complexities that were kept for later analysis.

5. Model Inspection

5.1 I-DEAS Debugging Tools

The finite element model of the PCU has been thoroughly debugged using tools provided by the I-DEAS software package.

Unconnected Nodes: All unconnected nodes have been removed from the model.

Coincident Nodes: There are no coincident nodes. The shortest distance between two nodes is 0.1mm, which is the smallest element size.

Coincident Elements: The model has been checked for overlaying and overlapping elements. All such coincident elements have been modified to form a unilayered mesh.

Free Element Edges: This is a test for element connectivity. All spurious free element edges have been eliminated ensuring all elements are properly joined. Appendix III contains images showing free element edges.

Interior Angles: All quadrilateral elements with an internal angle of 40^{o} or less have been replaced with triangular elements. These remain accurate in the model at small interior angles.

Distortion Order: The maximum distortion order found in the model is 0.56.

5.2 Mass Examination

5.2.1 Component Masses

Tabulated below is a mass breakdown of every component modeled as part of the finite element PCU model. The individual masses have been accurately gathered, but final mass of the assembled unit is likely to exceed this. Expected final weight is ca. 9.5 kg.

Table 2.

Component	No.	Each [kg]	Total [kg]
Radiator Plate	1	0.853	0.853
Connector Panel	1	0.631	0.631
Lid Plate	1	0.386	0.386
Base Plate	1	0.687	0.688
Vertical Shelf Assembly	1	0.160	0.160
Right Side Plate (-X)	1	0.802	0.803
Left Side Plate (+X)	1	0.936	0.937
Right Side Circuit Board	1	0.261	0.261
Left Side Circuit Board	1	0.261	0.261
Main Controller Board	1	0.340	0.340
CPU SPU Control Monitoring Board	1	0.142	0.142
AMUX Board	1	0.233	0.233
PCU Bracket Assembly	1	0.309	0.309
SPU Bracket Assembly	4	0.186	0.744

EMI FME Filter Module Assembly (MFL)	2	0.265	0.530
EMI FMC Filter Module Assembly (MTR)	6	0.190	1.140
Connectors	1	0.360	0.360
Main Controller Board Supports	3	0.019	0.057
AMUX Board Supports	6	0.003	0.018
Total			**8.850**

5.2.2 Centre of Mass

Centre of Mass:

$$X = 1.67 \cdot 10^{-1} m$$
$$Y = 7.68 \cdot 10^{-2} m$$
$$Z = -1.17 \cdot 10^{-1} m$$

The origin of the HIRDLS PCU model is the inside bottom right hand corner of the connector panel when looking at the connector panel from the outside. The axes are the finite element model axes as shown in the figures, not instrument axes. Images showing the position of the Centre of Mass can be found in Appendix III.

6. Model Evaluation

6.1 Boundary Conditions

The HIRDLS PCU is bolted to the main structure at six positions. This was modeled by applying boundary conditions to the nodes surrounding the six boltholes. These nodes are rigid in all six degrees of freedom. This is accurate on the premise that the main structure does not deform or provide extra support other than at the bolt locations.

Figure 1 below shows one of the six attachment locations. The blue ring of nodes around the bolthole is restrained.

Figure 1.

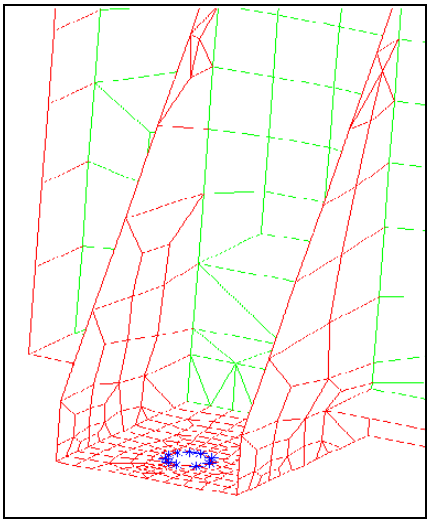

6.2 Static Load

Calculations for three static load cases were performed. This was done by applying a constant acceleration to the model. The axes are the finite element model axes as shown in the figures, not instrument axes.

Load Case 1: 50g along X-axis.
Load Case 2: 50g along Y-axis.
Load Case 3: 50g along Z-axis.

Table 3. Reaction Forces for Load Case 1 [N]

NODE	FORCE X	FORCE Y	FORCE Z		NODE	FORCE X	FORCE Y	FORCE Z
31	140.22	11.77	2.38		780	38.92	-126.59	40.50
32	-81.05	192.50	-2.54		781	80.76	-62.25	7.82
33	-63.88	-143.82	-3.05		782	-208.21	-102.09	155.22
34	-333.43	13.69	-8.17		783	-138.71	-139.65	130.91
74	124.69	-1.97	-74.84		784	-240.60	72.17	151.12
75	-71.82	120.22	53.62		794	84.66	158.57	-19.90
76	-47.04	-161.40	94.39		795	29.86	-75.74	2.36
77	-281.45	-43.74	177.36		796	76.56	-34.54	13.11
78	128.65	31.47	102.37		797	-207.77	-8.37	-140.71
79	-59.02	226.42	-110.17		798	-143.43	-54.16	-91.76
80	-55.92	-86.71	-41.17		799	-242.38	210.38	-211.85
81	-279.32	75.85	-197.26		834	89.40	145.40	-0.90
86	141.12	11.48	3.98		835	38.40	-119.48	4.31
87	-82.51	192.77	-2.53		836	89.37	-59.87	5.48
88	-64.58	-145.54	-2.35		837	-236.36	-68.38	-11.02
89	-337.12	12.20	-10.82		838	-171.15	-127.66	-9.63
130	127.57	-5.19	118.10		839	-289.39	152.99	-5.68
131	-74.40	114.01	-54.62		1088	70.34	91.28	19.58
132	-45.49	-172.39	-79.26		1089	41.66	-134.42	-22.17
133	-285.79	-55.21	-197.03		1090	83.53	-66.46	2.20
134	126.82	26.97	-73.19		1091	-210.68	-112.96	-165.87
135	-62.99	211.17	120.02		1092	-139.30	-151.18	-128.71
136	-56.05	-95.32	38.85		1093	-244.91	62.03	-168.79
137	-282.62	60.69	180.52		1103	80.90	149.24	35.34
506	89.23	145.02	5.41		1104	30.02	-81.56	0.09
507	38.20	-118.13	-3.98		1105	76.17	-37.82	-11.25
508	88.78	-59.09	-1.83		1106	-209.91	-19.77	126.31
509	-233.87	-66.80	-3.03		1107	-144.42	-64.16	82.85
510	-169.38	-125.79	-1.77		1108	-245.34	191.74	204.32
511	-286.11	153.57	-11.15					
779	69.84	94.63	-11.49		**Total**	**-4340.71**	**0.01**	**0.01**

Theoretical Results:

$$Force = Mass \cdot Acceleration$$

$$F = 8.85kg \cdot 50 \cdot 9.81ms^{-2} = 4340.9N$$

Theoretical and finite element model reaction forces are close to equal. This is an indicator of the model's accuracy. Tables of reaction forces for all load cases can be found in Appendix IV.

6.3 Dynamic Solution

Calculation of natural frequencies and corresponding mode shapes (normal modes) was performed using the Lanczos solver. This method is the preferred choice over Simultaneous Vector Iteration (SVI) and Guyan Reduction. The Lanczos solver is more economical than SVI methods and Guyan Reduction requires the user's choice of master degrees of freedom and is not useful for complicated simulations.

The normal modes for the unrestrained model were identified. The first six are the rigid body modes.

Mode 1: Frequency = 0.0 Hz
Mode 2: Frequency = 0.0 Hz
Mode 3: Frequency = 0.0 Hz
Mode 4: Frequency = 0.0 Hz
Mode 5: Frequency = 0.0 Hz
Mode 6: Frequency = 0.0 Hz
Mode 7: Frequency = 154.6 Hz

7. Analysis Results

7.1 Static Load

Tabulated below are the maximum stresses and displacements found in the metalwork for each of the load cases.

Table 4.

Load Case	Max. von Mises Stress $[Nm^{-2}]$	Max. Principle Stress $[Nm^{-2}]$	Max. Displacement $[m]$
1	$1.31 \cdot 10^{8}$	$8.27 \cdot 10^{7}$	$5.65 \cdot 10^{-4}$
2	$7.21 \cdot 10^{7}$	$4.45 \cdot 10^{7}$	$3.05 \cdot 10^{-4}$
3	$5.19 \cdot 10^{7}$	$3.99 \cdot 10^{7}$	$4.25 \cdot 10^{-4}$

The highest stress due to a 50g acceleration is $\sigma_{\max} = 1.31 \cdot 10^{8}\, Nm^{-2}$. This is considerably less than the 0.2% Proof Stress of $\sigma_{y_{0.2\%}} = 2.7 \cdot 10^{8}\, Nm^{-2}$ and the Ultimate Tensile Stress of $\sigma_{UTS} = 3.1 \cdot 10^{8}\, Nm^{-2}$. Working to a yield safety factor YSF=1.25, a Yield Margin of Safety

$$
\begin{aligned}
MoS_{Yield} &= \frac{\sigma_{allowable}}{\sigma_{applied} \cdot YSF} - 1 \\
&= \frac{\sigma_{y_{0.2\%}}}{\sigma_{\max} \cdot YSF} - 1 \\
&= \frac{2.7 \cdot 10^{8}}{1.31 \cdot 10^{8} \cdot 1.25} - 1 \\
&= 0.65
\end{aligned}
$$

is reached.

Working to an ultimate safety factor USF=1.4, an Ultimate Margin of Safety

$$
\begin{aligned}
MoS_{Ultimate} &= \frac{\sigma_{allowable}}{\sigma_{applied} \cdot USF} - 1 \\
&= \frac{\sigma_{UTS}}{\sigma_{\max} \cdot USF} - 1 \\
&= \frac{3.1 \cdot 10^{8}}{1.31 \cdot 10^{8} \cdot 1.4} - 1 \\
&= 0.69
\end{aligned}
$$

is reached.

Images of stress distributions for all components can be found in Appendix V.

7.2 Dynamic Solution

Table 5 below summarizes the first ten normal modes identified. The lowest natural frequency of 153.55Hz far exceeds the minimum allowed. Appendix VI contains images of the first ten normal mode shapes.

Table 5.

Mode	Freq. [Hz]	Resonant Components	Mode No.
1	153.55	PCU/SPU Control Monitoring Board	1st mode
2	170.35	Connector Panel	1st mode
3	190.63	PCU/SPU Control Monitoring Board	2nd mode
4	197.67	Connector Panel	2nd mode
5	202.18	Side Plates Top Plate Connector Panel	1st mode 1st mode 2nd mode
6	209.30	Side Plates Top Plate Connector Panel	1st mode 1st mode 2nd mode
7	234.97	PCU Bracket PCU/SPU Control Monitoring Board	1st mode 3rd mode
8	238.18	Side Panels	2nd mode
9	240.58	Side Panels	2nd mode
10	253.99	Lid Panel Base Plate	1st mode 1st mode

8. Comments

The results of this analysis only give a general indication of the mechanical behavior of the PCU. Finite element methods are intrinsically imprecise due to the selection of a finite number of elements. Processing power limits the number of model elements. Inaccuracies are also introduced during the selection of the solution method (Lanczos vs. SVI, Guyan Reduction), numerical limitations of computers and most importantly the approximations made at the start of and during the model creation.

However, if adequate margins of safety are applied to the results, the method is sufficiently accurate to ensure failure in service is unlikely to occur.

This analysis can be assumed valid because the results have a large margin of safety. The factors that introduce inaccuracies mentioned above have been taken into consideration:

1. The approximations made at the start of and during the model creation are realistic and veer towards a worst case rather than an optimistic scenario.

2. Numerical limitations of computers are unavoidable but are negligible compared to other sources of imprecision.

3. The Lanczos solver was chosen as the optimal solution method available for this analysis under I-DEAS.

4. The number of elements created was the maximum with respect to processing power available. Areas of particular interest such as high stress zones were modeled in more detail.

9. Conclusions

1. The maximum expected material stress is $1.31 \cdot 10^{8} Nm^{-2}$. This is within acceptable material allowable limits.

2. The maximum expected deflection is $5.56 \cdot 10^{-4} m$. This is within the geometric limitation placed on the HIRDLS PCU.

3. The first natural frequency of the HIRDLS PCU is 153.55Hz. This is above the 100Hz requirement not to cause resonance of the HIRDLS main structure.

4. Despite the idealistic nature of the modeling, the results give a valid indication of the mechanical behavior of the PCU.

10. Appendix

Appendix I: HIRDLS PCU Solid

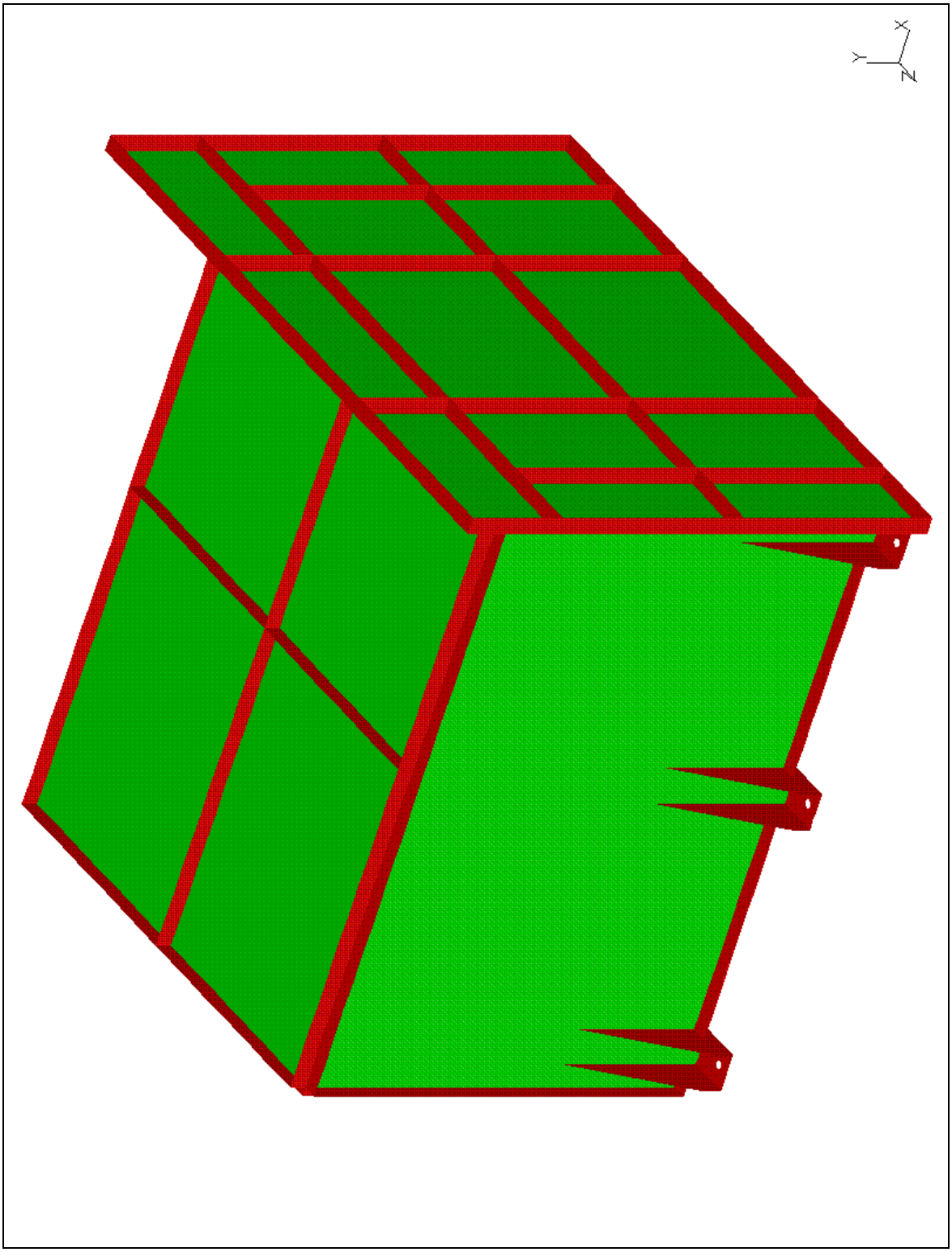

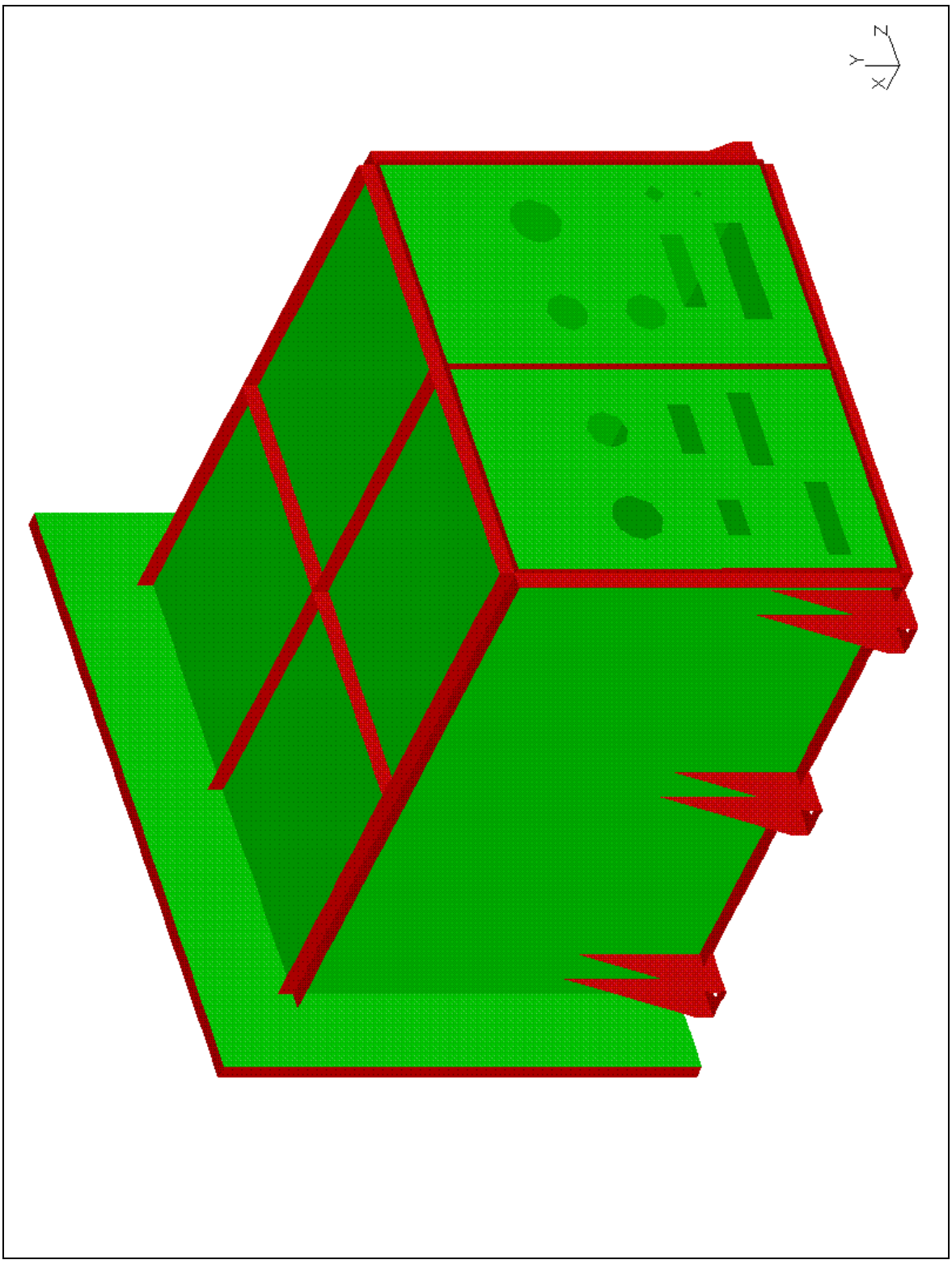
Z
Y
X

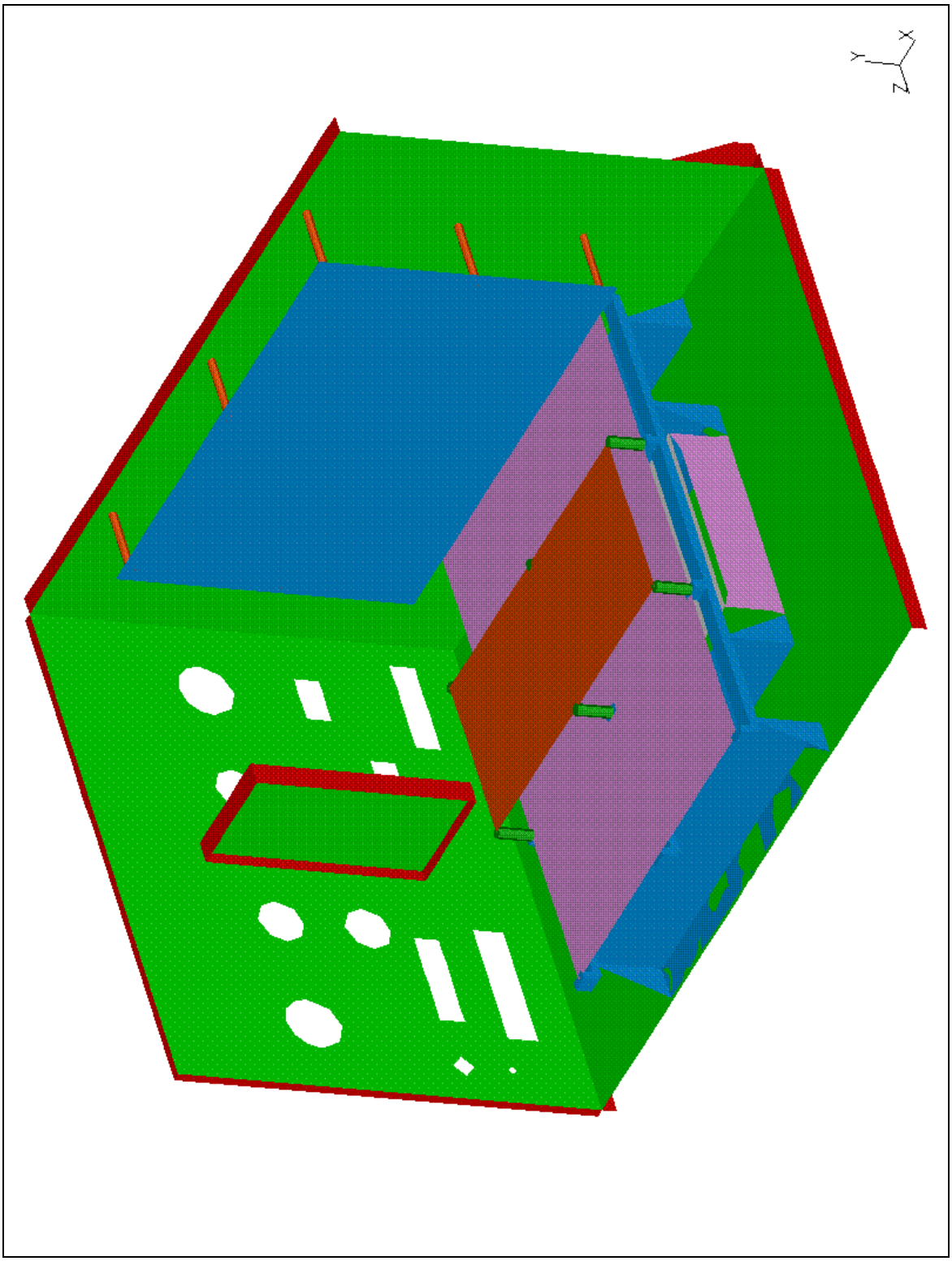
X
Y
Z

Appendix II: HIRDLS PCU Mesh

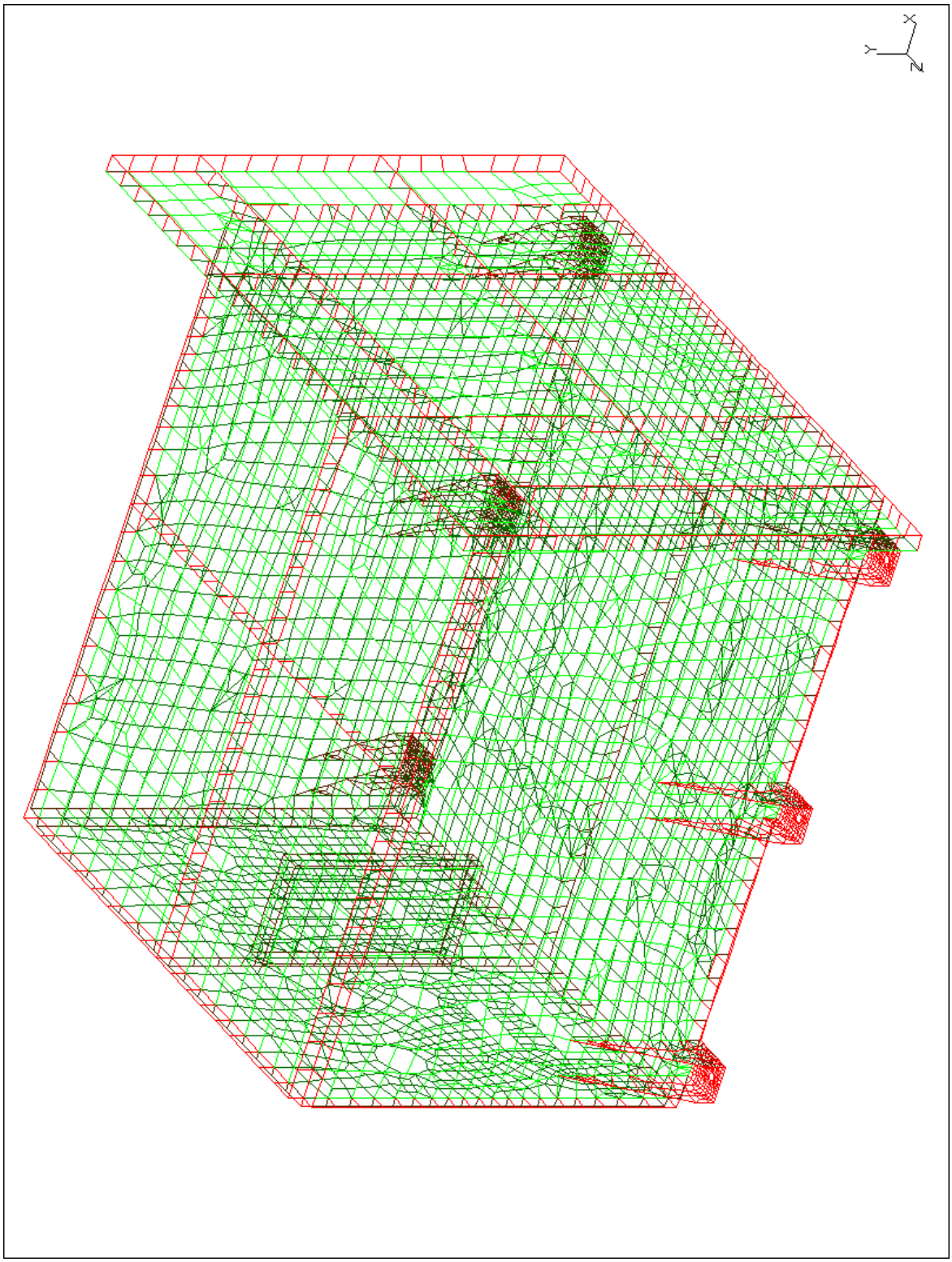

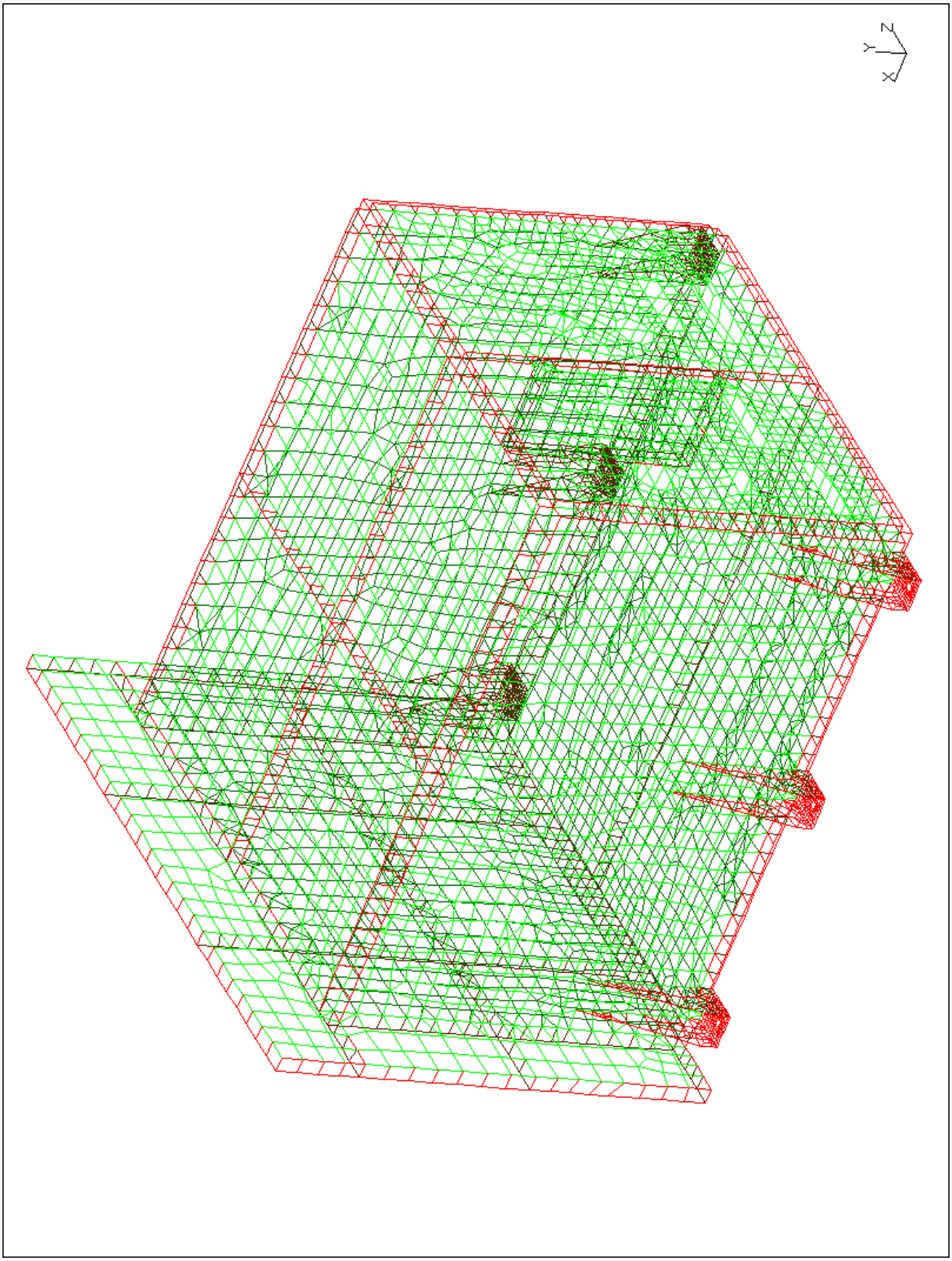
Z
Y
X

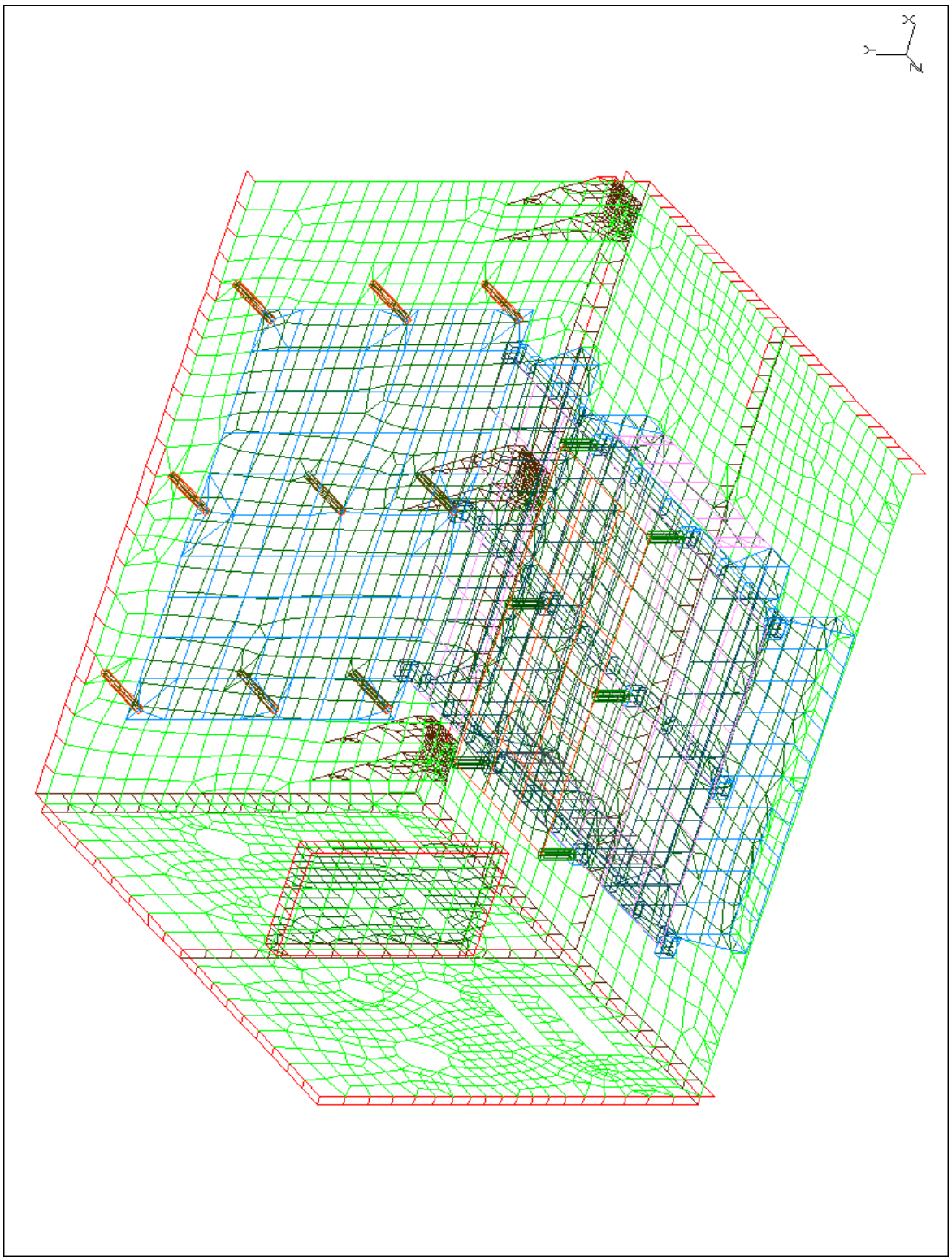
X
Y
Z

Appendix III: Free Element Edges/Centre of Mass

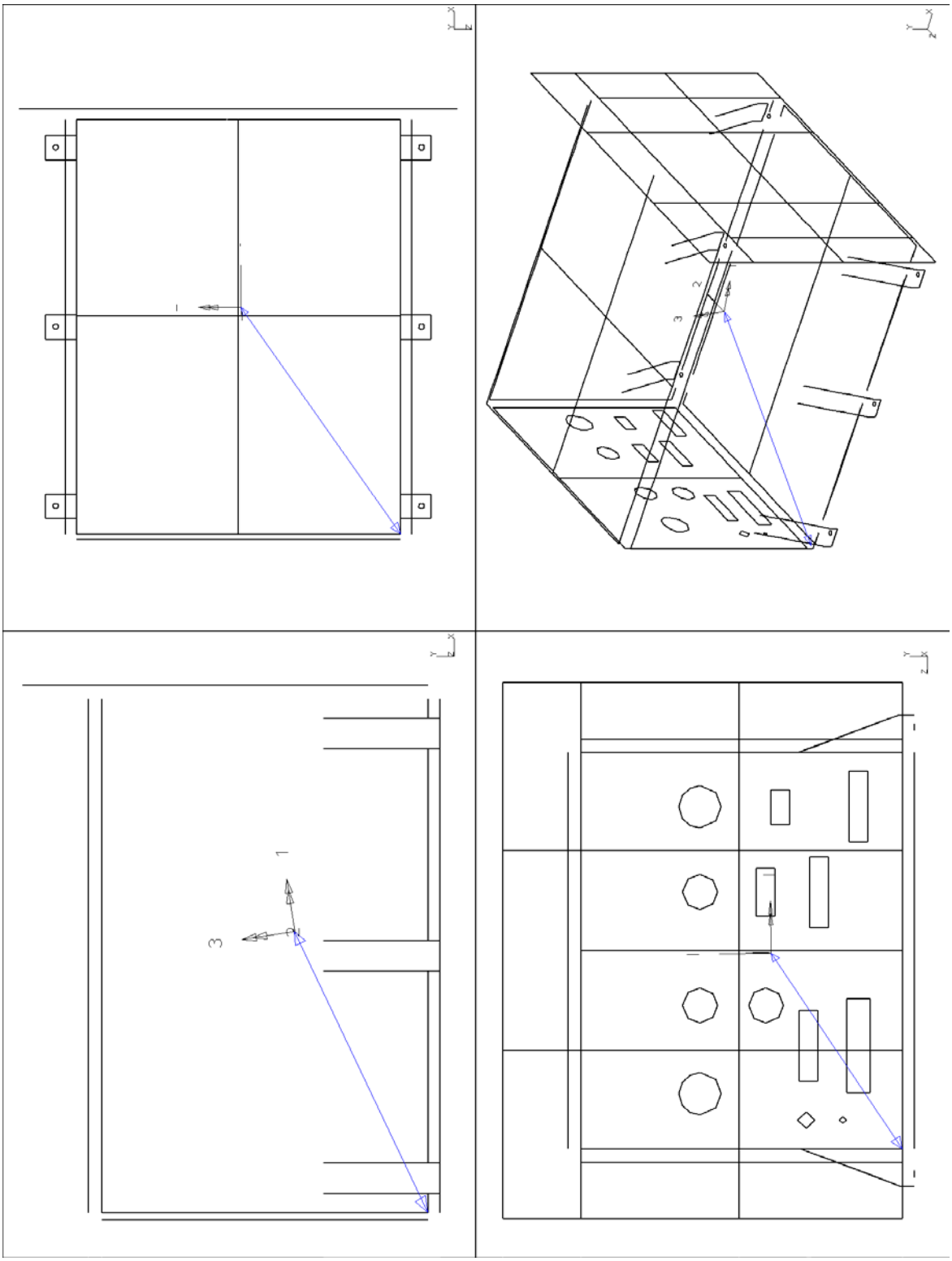

Appendix IV: Reaction Forces

Reaction Forces for Load Case 1 [N]

NODE	FORCE X	FORCE Y	FORCE Z		NODE	FORCE X	FORCE Y	FORCE Z
31	140.22	11.77	2.38		780	38.92	-126.59	40.50
32	-81.05	192.50	-2.54		781	80.76	-62.25	7.82
33	-63.88	-143.82	-3.05		782	-208.21	-102.09	155.22
34	-333.43	13.69	-8.17		783	-138.71	-139.65	130.91
74	124.69	-1.97	-74.84		784	-240.60	72.17	151.12
75	-71.82	120.22	53.62		794	84.66	158.57	-19.90
76	-47.04	-161.40	94.39		795	29.86	-75.74	2.36
77	-281.45	-43.74	177.36		796	76.56	-34.54	13.11
78	128.65	31.47	102.37		797	-207.77	-8.37	-140.71
79	-59.02	226.42	-110.17		798	-143.43	-54.16	-91.76
80	-55.92	-86.71	-41.17		799	-242.38	210.38	-211.85
81	-279.32	75.85	-197.26		834	89.40	145.40	-0.90
86	141.12	11.48	3.98		835	38.40	-119.48	4.31
87	-82.51	192.77	-2.53		836	89.37	-59.87	5.48
88	-64.58	-145.54	-2.35		837	-236.36	-68.38	-11.02
89	-337.12	12.20	-10.82		838	-171.15	-127.66	-9.63
130	127.57	-5.19	118.10		839	-289.39	152.99	-5.68
131	-74.40	114.01	-54.62		1088	70.34	91.28	19.58
132	-45.49	-172.39	-79.26		1089	41.66	-134.42	-22.17
133	-285.79	-55.21	-197.03		1090	83.53	-66.46	2.20
134	126.82	26.97	-73.19		1091	-210.68	-112.96	-165.87
135	-62.99	211.17	120.02		1092	-139.30	-151.18	-128.71
136	-56.05	-95.32	38.85		1093	-244.91	62.03	-168.79
137	-282.62	60.69	180.52		1103	80.90	149.24	35.34
506	89.23	145.02	5.41		1104	30.02	-81.56	0.09
507	38.20	-118.13	-3.98		1105	76.17	-37.82	-11.25
508	88.78	-59.09	-1.83		1106	-209.91	-19.77	126.31
509	-233.87	-66.80	-3.03		1107	-144.42	-64.16	82.85
510	-169.38	-125.79	-1.77		1108	-245.34	191.74	204.32
511	-286.11	153.57	-11.15					
779	69.84	94.63	-11.49		**Total**	**-4340.71**	**0.01**	**0.01**

Reaction Forces for Load Case 2 [N]

NODE	FORCE X	FORCE Y	FORCE Z		NODE	FORCE X	FORCE Y	FORCE Z
31	2.97	22.74	-72.17		780	-18.17	68.11	-38.29
32	1.50	74.89	-63.62		781	-12.06	35.54	-15.31
33	-1.84	50.97	-57.23		782	-23.81	102.88	-34.74
34	-1.60	70.73	13.58		783	-20.23	105.49	-42.41
74	-4.76	38.58	-99.17		784	-39.80	143.80	-61.06
75	-10.33	114.04	-74.35		794	17.55	67.30	-36.52
76	-19.85	97.50	-49.03		795	-3.40	50.65	-50.35
77	-34.36	124.42	-39.77		796	-1.60	26.90	-24.00
78	6.46	33.21	-103.17		797	16.35	82.87	-19.24
79	16.26	110.21	-39.49		798	10.11	78.13	-36.89
80	2.68	72.01	-55.18		799	9.73	130.99	-26.21
81	20.08	106.48	-15.00		834	5.67	41.91	107.15
86	-1.20	22.09	78.86		835	-5.76	38.85	66.19
87	2.71	67.92	78.49		836	-5.57	22.74	60.11
88	-0.42	54.75	50.19		837	4.20	55.17	-8.50
89	6.37	68.80	-17.76		838	5.99	61.08	17.92
130	-3.22	32.25	110.29		839	-2.85	81.09	18.99
131	-3.92	95.61	74.02		1088	3.71	58.39	70.43
132	-12.30	81.72	27.73		1089	-13.34	57.37	26.12
133	-16.86	103.51	12.02		1090	-9.29	29.86	10.95
134	8.28	38.99	105.50		1091	-10.87	85.91	7.99
135	26.75	129.53	59.36		1092	-10.15	87.82	17.25
136	8.49	84.69	60.01		1093	-23.23	119.42	42.27
137	40.67	125.81	33.99		1103	23.43	78.80	47.28
506	8.84	46.86	-90.49		1104	-1.72	59.77	51.57
507	-4.46	35.66	-70.65		1105	-0.97	31.80	23.36
508	-2.92	21.23	-60.39		1106	31.68	98.17	31.68
509	-1.55	54.15	2.13		1107	20.71	91.57	45.31
510	1.83	58.14	-25.86		1108	26.77	153.79	51.46
511	-9.48	87.45	-13.79					
779	2.09	69.65	-61.56		**Total**	**0.00**	**4340.70**	**0.01**

Reaction Forces for Load Case 3 [N]

NODE	FORCE X	FORCE Y	FORCE Z		NODE	FORCE X	FORCE Y	FORCE Z
31	-3.19	18.98	51.91		780	-9.60	42.21	-57.54
32	9.44	56.34	-56.84		781	-9.22	22.38	-14.98
33	-1.94	48.89	-45.60		782	7.85	66.41	-179.26
34	14.24	72.81	-173.65		783	2.36	65.16	-153.76
74	-7.58	21.95	69.11		784	5.48	84.85	-187.31
75	7.47	61.68	-72.61		794	5.87	36.35	-31.48
76	-4.59	60.16	-117.53		795	-6.64	31.37	-5.70
77	10.77	79.05	-209.29		796	-3.35	16.79	8.85
78	1.07	19.52	65.46		797	-5.53	55.16	-127.28
79	2.52	60.14	-104.54		798	-6.54	52.47	-89.85
80	-7.57	46.21	-47.45		799	-9.00	78.35	-181.42
81	-7.14	68.60	-169.81		834	-10.08	-41.55	26.47
86	-5.24	-19.80	53.16		835	4.49	-26.71	7.95
87	-3.28	-67.98	-63.76		836	0.28	-16.45	34.52
88	6.93	-40.58	-43.27		837	9.22	-54.15	-128.32
89	9.07	-73.89	-179.90		838	6.57	-52.83	-99.87
130	0.52	-19.45	69.51		839	11.04	-87.89	-168.92
131	-10.12	-60.57	-64.99		1088	-7.20	-35.69	5.19
132	1.99	-46.13	-81.83		1089	5.07	-31.96	-34.95
133	-11.54	-68.98	-172.80		1090	3.88	-17.26	-6.44
134	-9.47	-23.21	69.89		1091	-8.10	-55.03	-142.31
135	-6.25	-79.74	-155.65		1092	-3.11	-51.28	-115.63
136	5.81	-45.62	-57.11		1093	-7.28	-78.92	-160.35
137	6.88	-79.88	-220.72		1103	-13.96	-49.20	-57.38
506	5.10	32.68	29.32		1104	3.09	-30.34	-5.31
507	-6.28	33.64	4.60		1105	-1.78	-16.56	12.60
508	-5.51	19.93	31.92		1106	5.32	-60.26	-160.44
509	7.14	57.81	-125.75		1107	6.23	-53.72	-110.97
510	5.40	59.98	-99.87		1108	9.30	-98.11	-248.26
511	8.96	78.46	-159.71					
779	1.73	35.44	9.23		**Total**	**0.00**	**0.00**	**-4340.71**

Appendix V: Stresses

Load Case 1

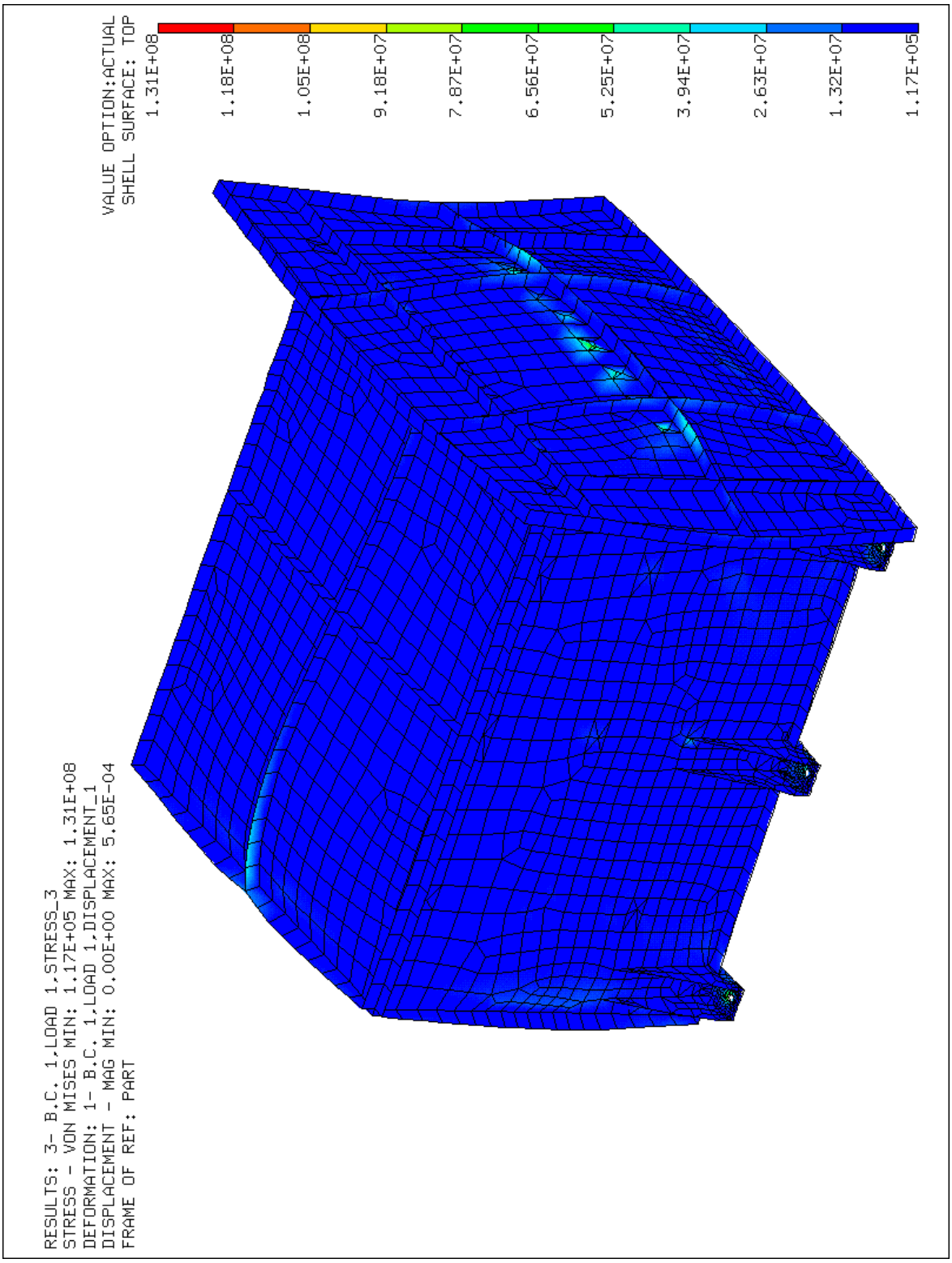

Load Case 2

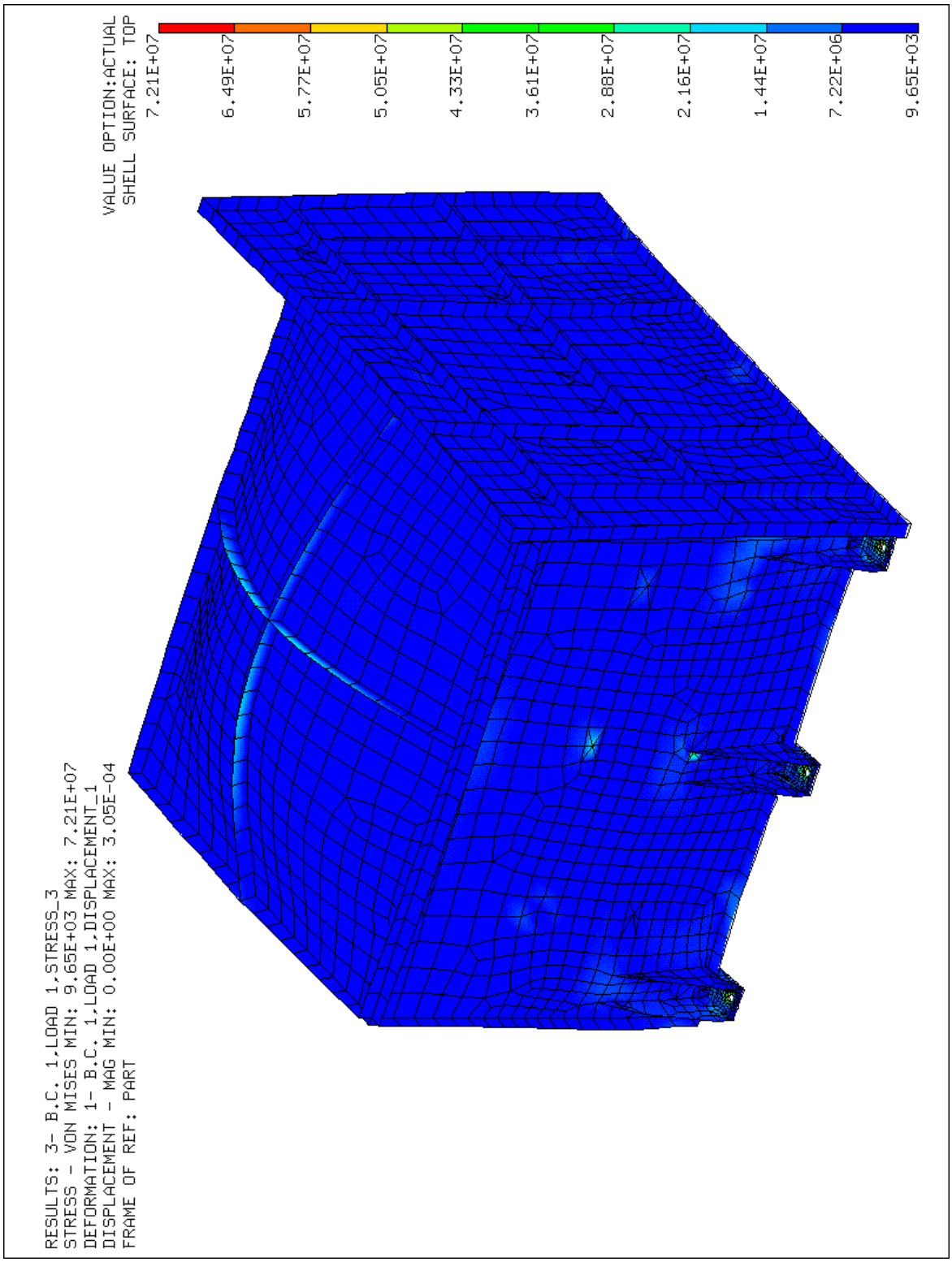
VALUE OPTION:ACTUAL
SHELL SURFACE: TOP
7.21E+07
6.49E+07
5.77E+07
5.05E+07
4.33E+07
3.61E+07
2.88E+07
2.16E+07
1.44E+07
7.22E+06
9.65E+03
RESULTS: 3- B.C. 1,LOAD 1,STRESS_3
STRESS - VON MISES MIN: 9.65E+03 MAX: 7.21E+07
DEFORMATION: 1- B.C. 1,LOAD 1,DISPLACEMENT_1
DISPLACEMENT - MAG MIN: 0.00E+00 MAX: 3.05E-04
FRAME OF REF: PART

Load Case 3

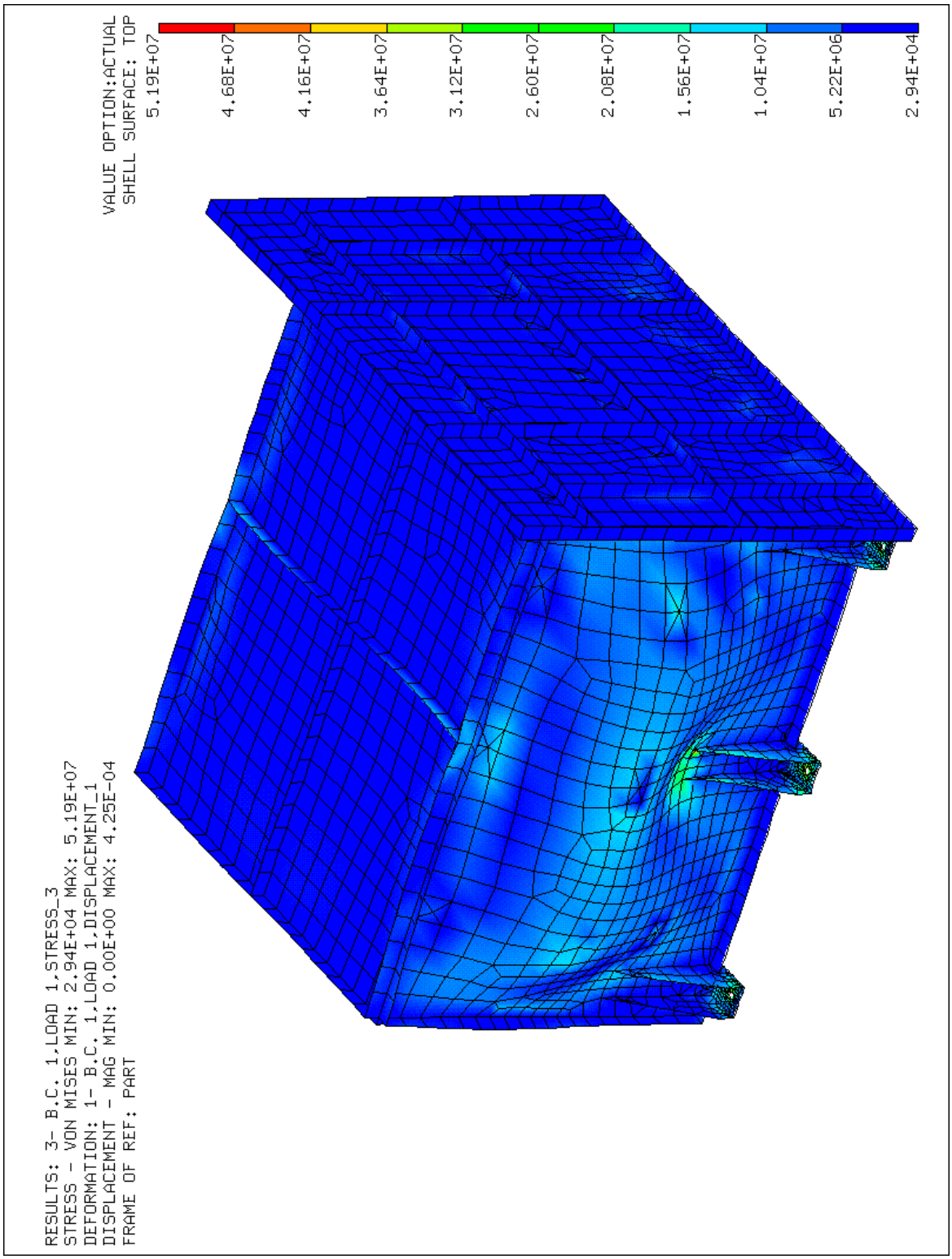
VALUE OPTION:ACTUAL
SHELL SURFACE: TOP
5.19E+07
4.68E+07
4.16E+07
3.64E+07
3.12E+07
2.60E+07
2.08E+07
1.56E+07
1.04E+07
5.22E+06
2.94E+04
RESULTS: 3- B.C. 1,LOAD 1,STRESS_3
STRESS - VON MISES MIN: 2.94E+04 MAX: 5.19E+07
DEFORMATION: 1- B.C. 1,LOAD 1,DISPLACEMENT_1
DISPLACEMENT - MAG MIN: 0.00E+00 MAX: 4.25E-04
FRAME OF REF: PART

Maximum Stress:

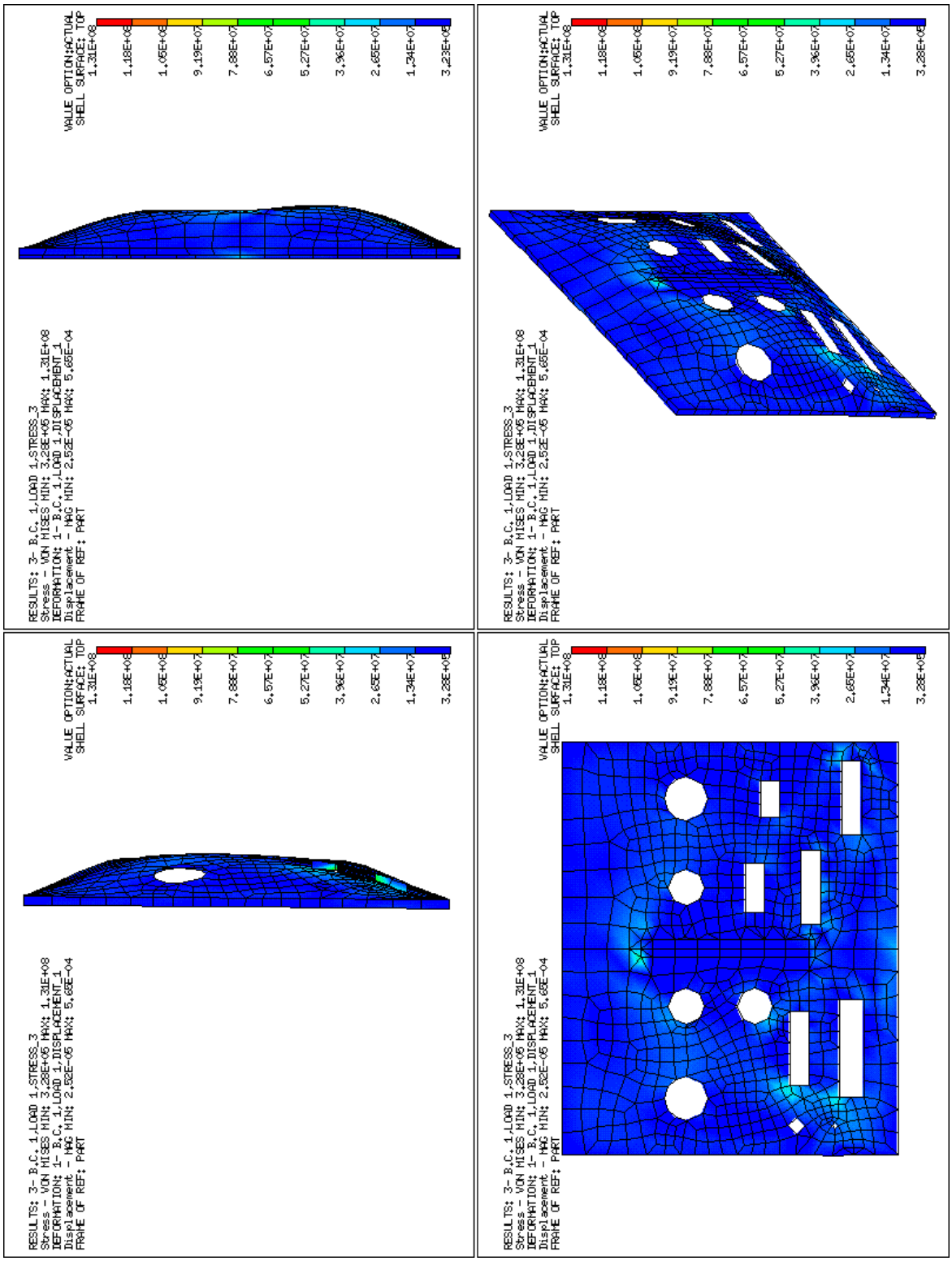

Appendix VI: Mode Shapes

Mode 1

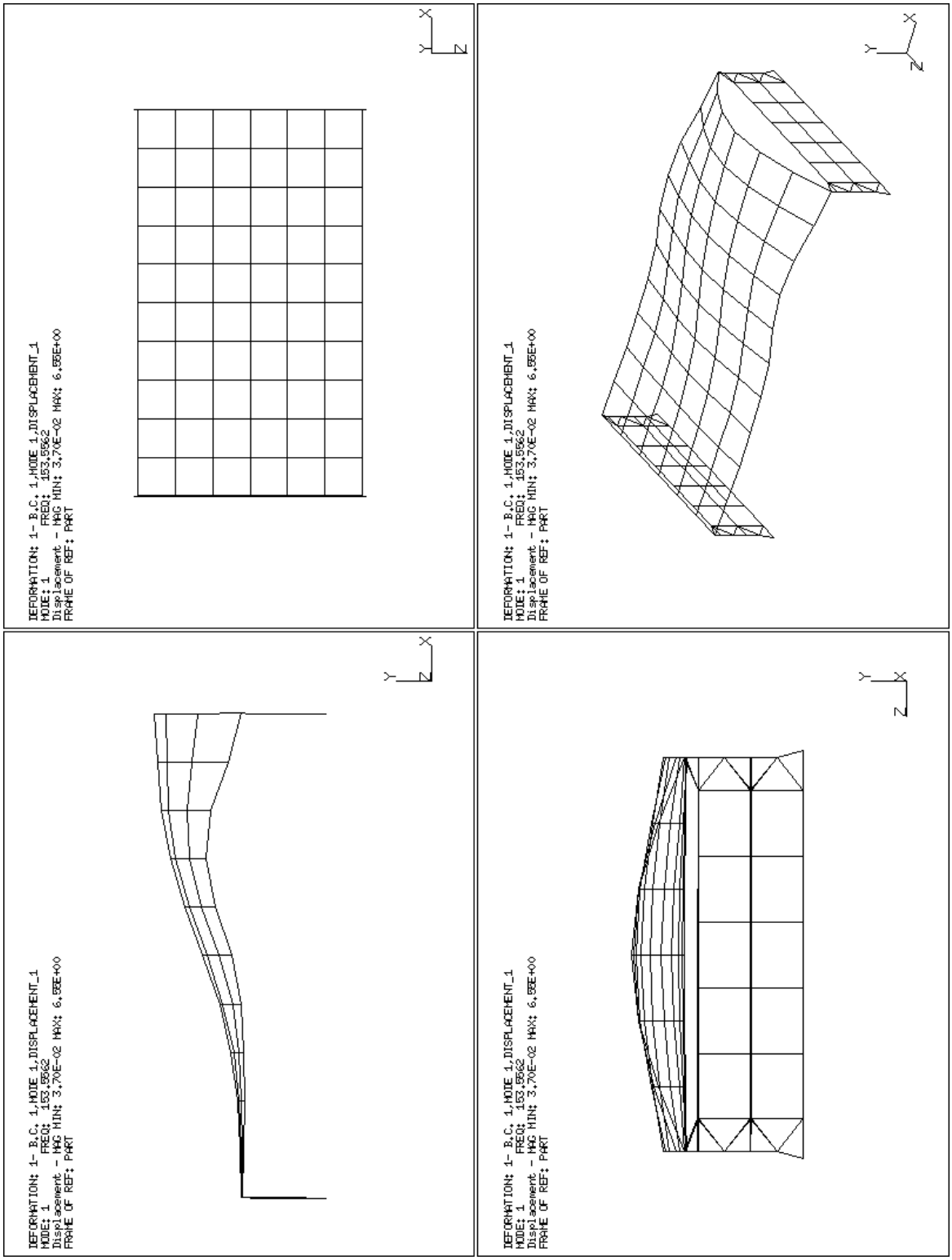

Mode 2

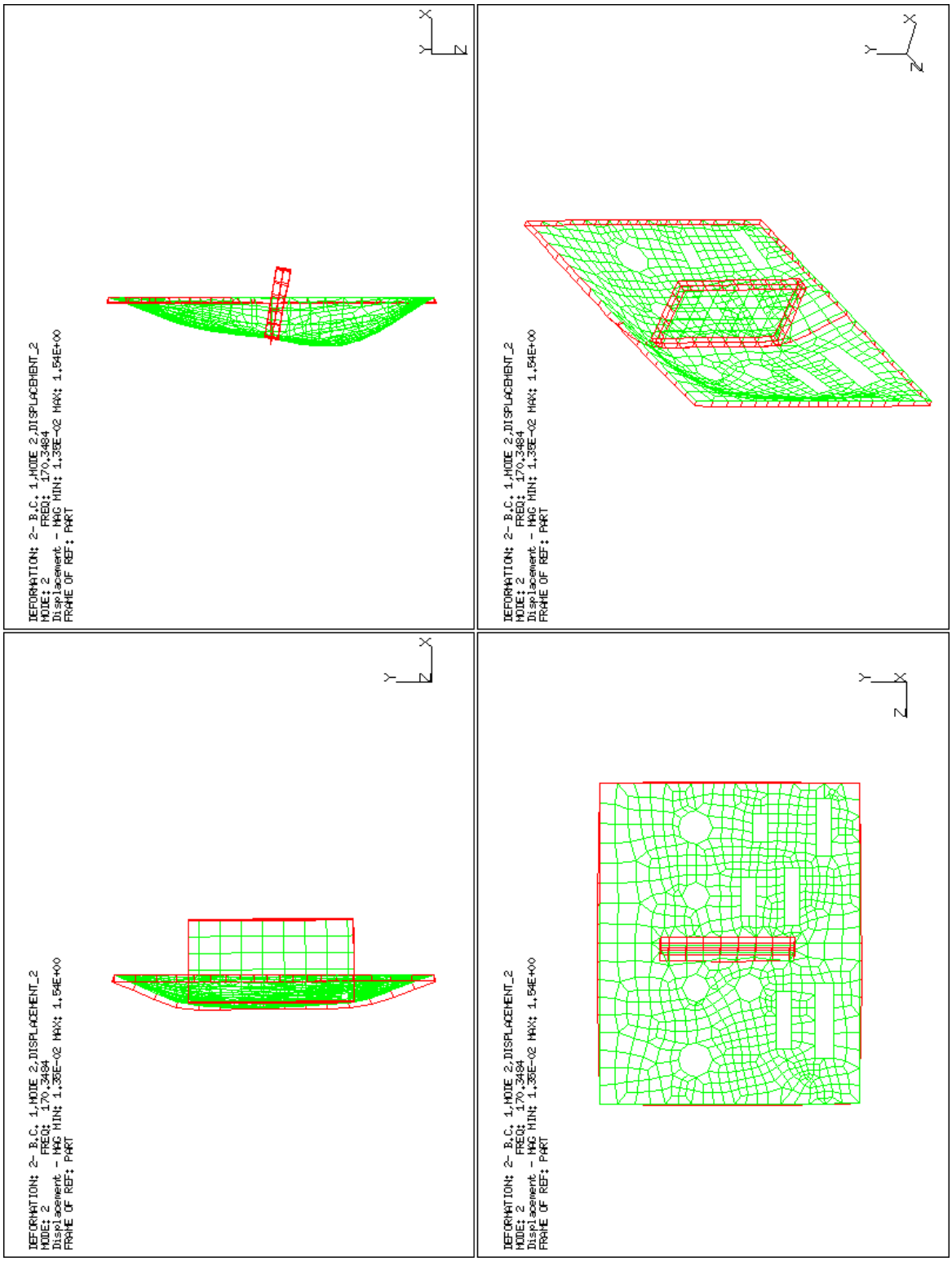
DEFORMATION: 2- B.C. 1,MODE 2,DISPLACEMENT_2
MODE: 2 FREQ: 170.3484
Displacement - MAG MIN: 1.38E-02 MAX: 1.54E+00
FRAME OF REF: PART

Mode 3

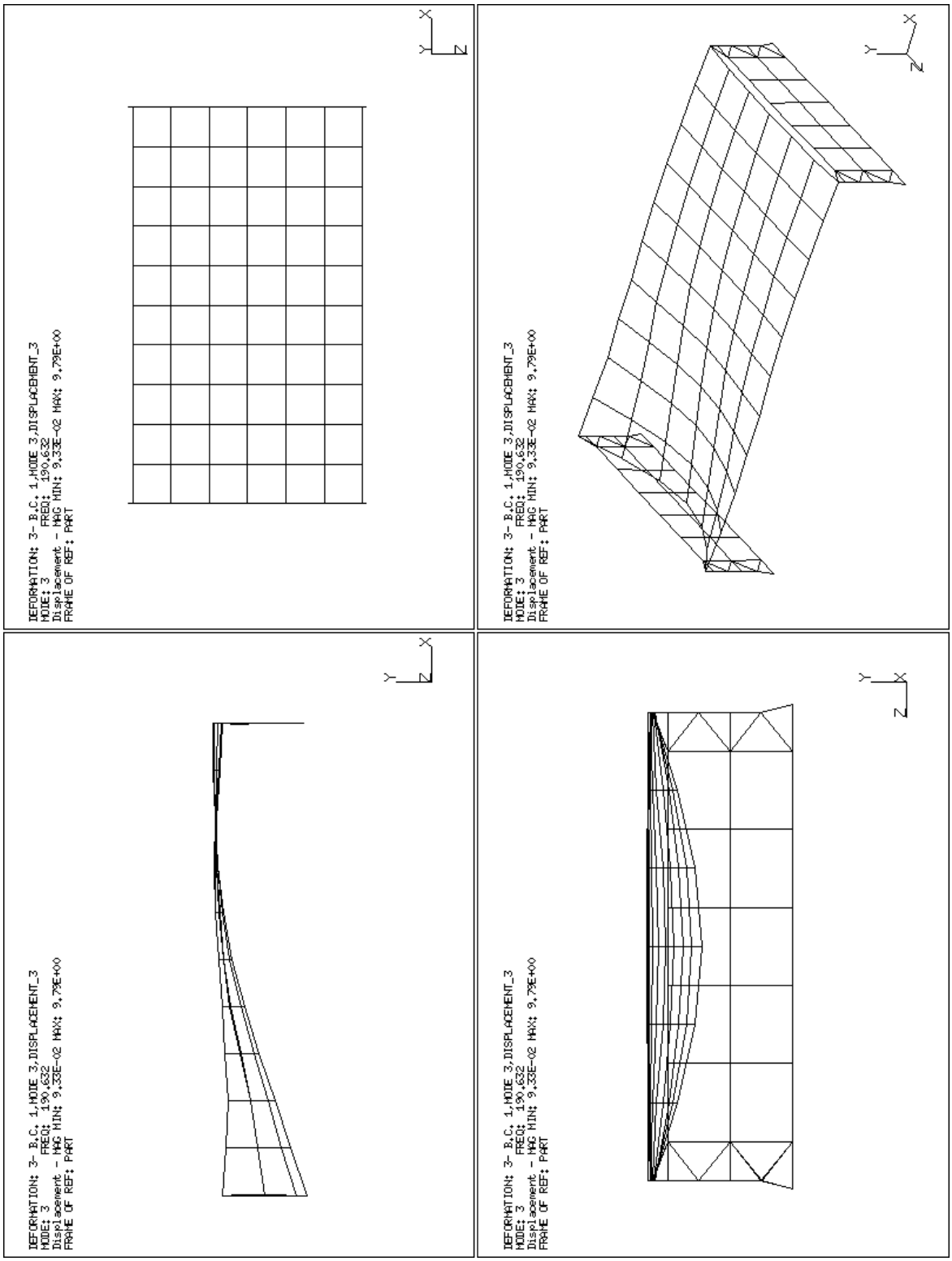
DEFORMATION: 3- B.C. 1,MODE 3,DISPLACEMENT_3
MODE: 3 FREQ: 190.632
Displacement - MAG MIN: 9.33E-02 MAX: 9.79E+00
FRAME OF REF: PART
DEFORMATION: 3- B.C. 1,MODE 3,DISPLACEMENT_3
MODE: 3 FREQ: 190.632
Displacement - MAG MIN: 9.33E-02 MAX: 9.79E+00
FRAME OF REF: PART
DEFORMATION: 3- B.C. 1,MODE 3,DISPLACEMENT_3
MODE: 3 FREQ: 190.632
Displacement - MAG MIN: 9.33E-02 MAX: 9.79E+00
FRAME OF REF: PART
DEFORMATION: 3- B.C. 1,MODE 3,DISPLACEMENT_3
MODE: 3 FREQ: 190.632
Displacement - MAG MIN: 9.33E-02 MAX: 9.79E+00
FRAME OF REF: PART

Mode 4

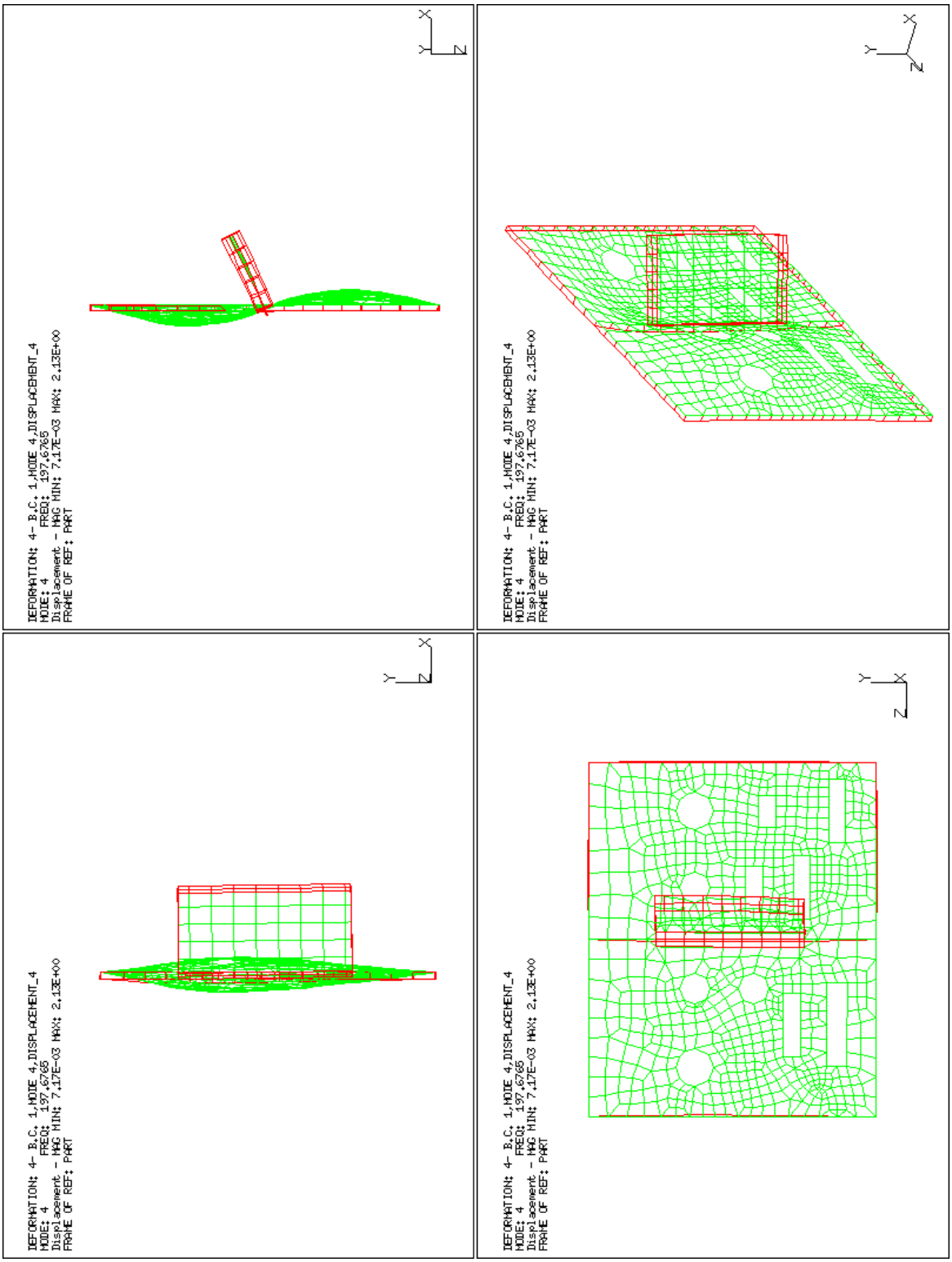
DEFORMATION: 4- B.C. 1,MODE 4,DISPLACEMENT_4
MODE: 4 FREQ: 197.6765
Displacement - MAG MIN: 7.17E-03 MAX: 2.13E+00
FRAME OF REF: PART
DEFORMATION: 4- B.C. 1,MODE 4,DISPLACEMENT_4
MODE: 4 FREQ: 197.6765
Displacement - MAG MIN: 7.17E-03 MAX: 2.13E+00
FRAME OF REF: PART
DEFORMATION: 4- B.C. 1,MODE 4,DISPLACEMENT_4
MODE: 4 FREQ: 197.6765
Displacement - MAG MIN: 7.17E-03 MAX: 2.13E+00
FRAME OF REF: PART
DEFORMATION: 4- B.C. 1,MODE 4,DISPLACEMENT_4
MODE: 4 FREQ: 197.6765
Displacement - MAG MIN: 7.17E-03 MAX: 2.13E+00
FRAME OF REF: PART

Mode 5

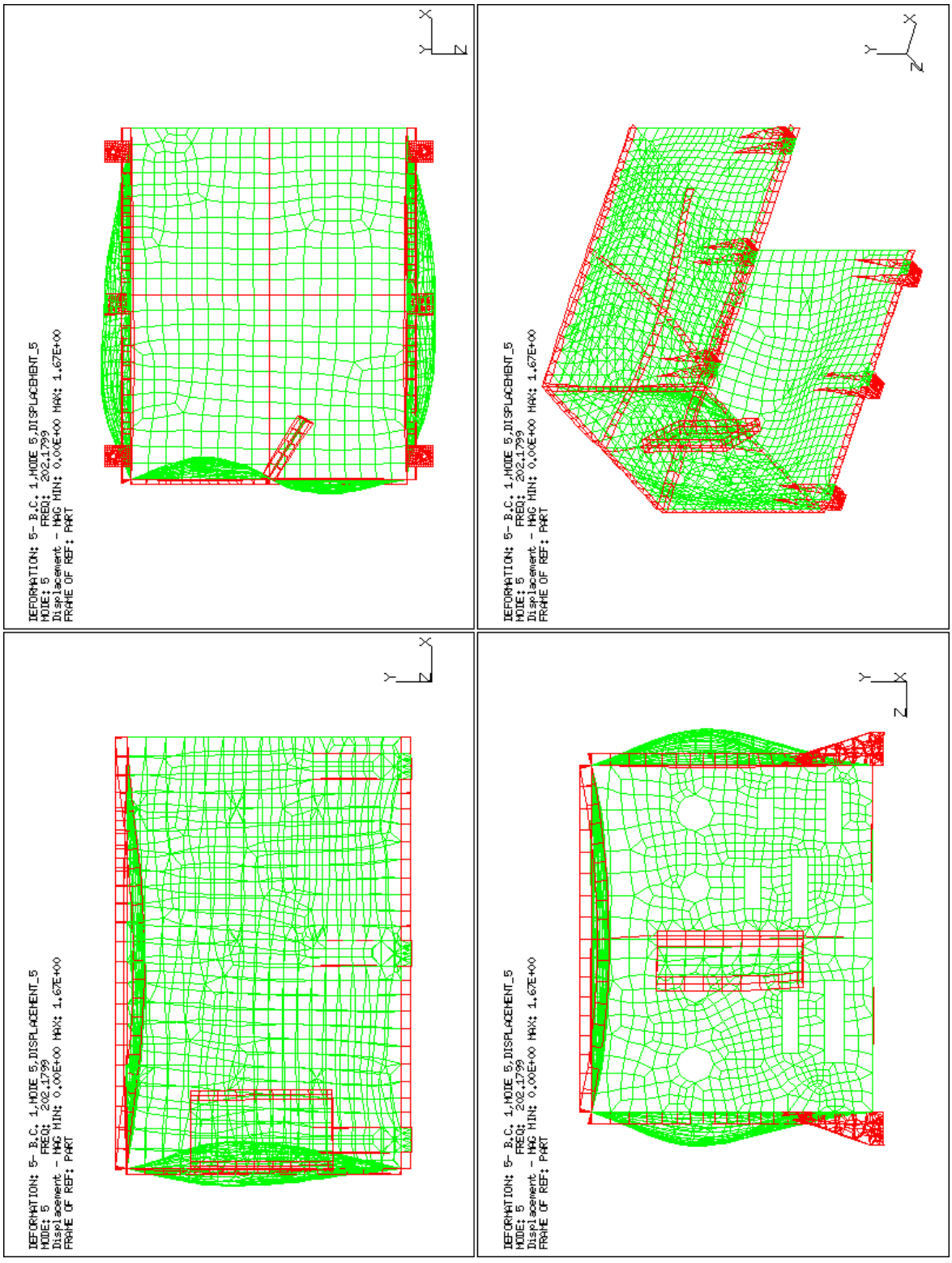
DEFORMATION: 5- B.C. 1,MODE 5,DISPLACEMENT_5
MODE: 5
FREQ: 202.1799
Displacement - MAG MIN: 0.00E+00 MAX: 1.67E+00
FRAME OF REF: PART

Mode 6

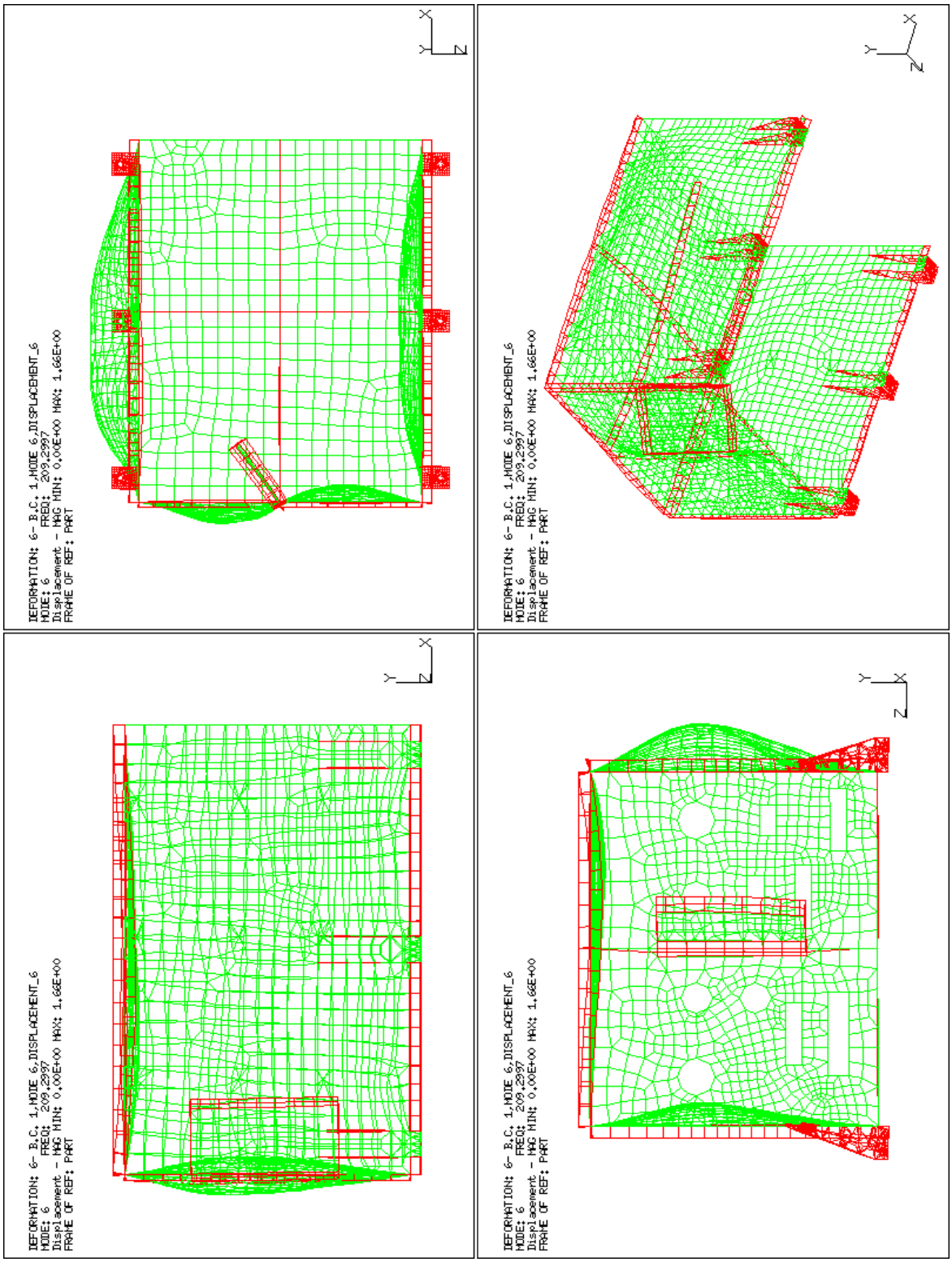
DEFORMATION: 6- B.C.: 1,MODE 6,DISPLACEMENT_6
MODE: 6 FREQ: 209,2997
Displacement - MAG MIN: 0,00E+00 MAX: 1,66E+00
FRAME OF REF: PART

Mode 7

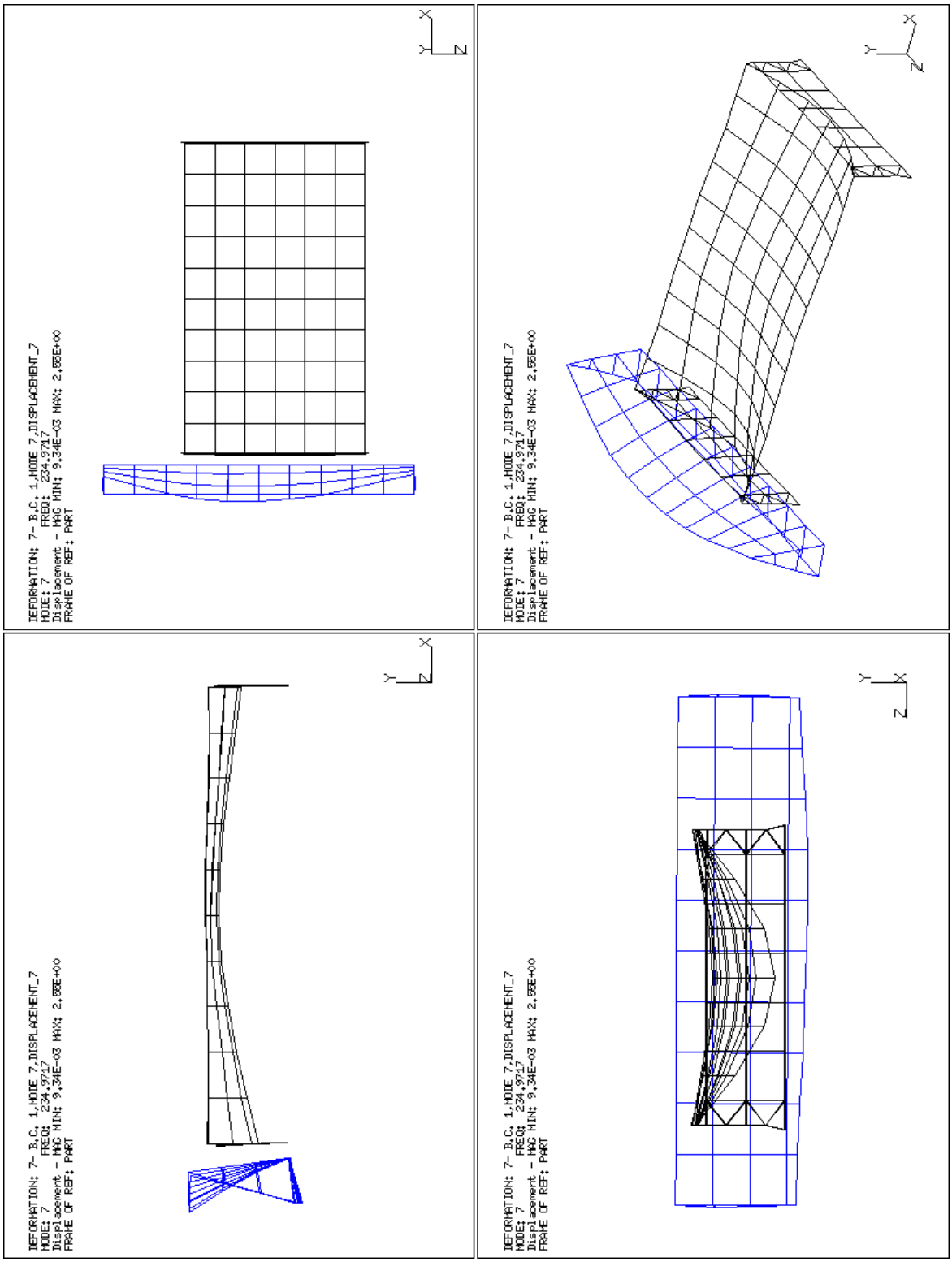
DEFORMATION: 7- B.C. 1,MODE 7,DISPLACEMENT_7
MODE: 7 FREQ: 234,9717
Displacement - MAG MIN: 9,34E-03 MAX: 2,88E+00
FRAME OF REF: PART
DEFORMATION: 7- B.C. 1,MODE 7,DISPLACEMENT_7
MODE: 7 FREQ: 234,9717
Displacement - MAG MIN: 9,34E-03 MAX: 2,88E+00
FRAME OF REF: PART
DEFORMATION: 7- B.C. 1,MODE 7,DISPLACEMENT_7
MODE: 7 FREQ: 234,9717
Displacement - MAG MIN: 9,34E-03 MAX: 2,88E+00
FRAME OF REF: PART
DEFORMATION: 7- B.C. 1,MODE 7,DISPLACEMENT_7
MODE: 7 FREQ: 234,9717
Displacement - MAG MIN: 9,34E-03 MAX: 2,88E+00
FRAME OF REF: PART

Mode 8

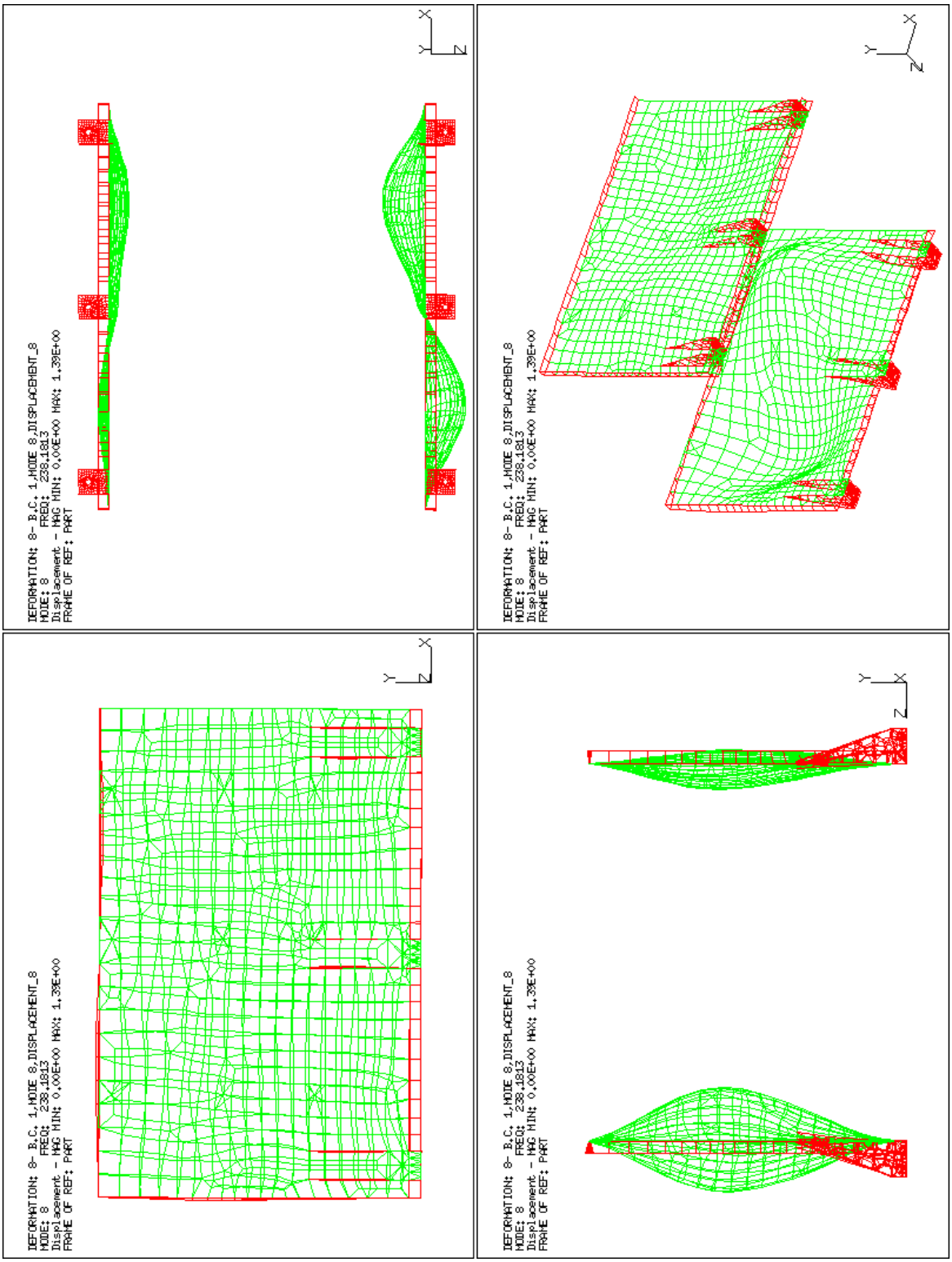
DEFORMATION: 8- B.C. 1,MODE 8,DISPLACEMENT_8
MODE: 8 FREQ: 238.1813
Displacement - MAG MIN: 0.00E+00 MAX: 1.39E+00
FRAME OF REF: PART
DEFORMATION: 8- B.C. 1,MODE 8,DISPLACEMENT_8
MODE: 8 FREQ: 238.1813
Displacement - MAG MIN: 0.00E+00 MAX: 1.39E+00
FRAME OF REF: PART
DEFORMATION: 8- B.C. 1,MODE 8,DISPLACEMENT_8
MODE: 8 FREQ: 238.1813
Displacement - MAG MIN: 0.00E+00 MAX: 1.39E+00
FRAME OF REF: PART
DEFORMATION: 8- B.C. 1,MODE 8,DISPLACEMENT_8
MODE: 8 FREQ: 238.1813
Displacement - MAG MIN: 0.00E+00 MAX: 1.39E+00
FRAME OF REF: PART

Mode 9

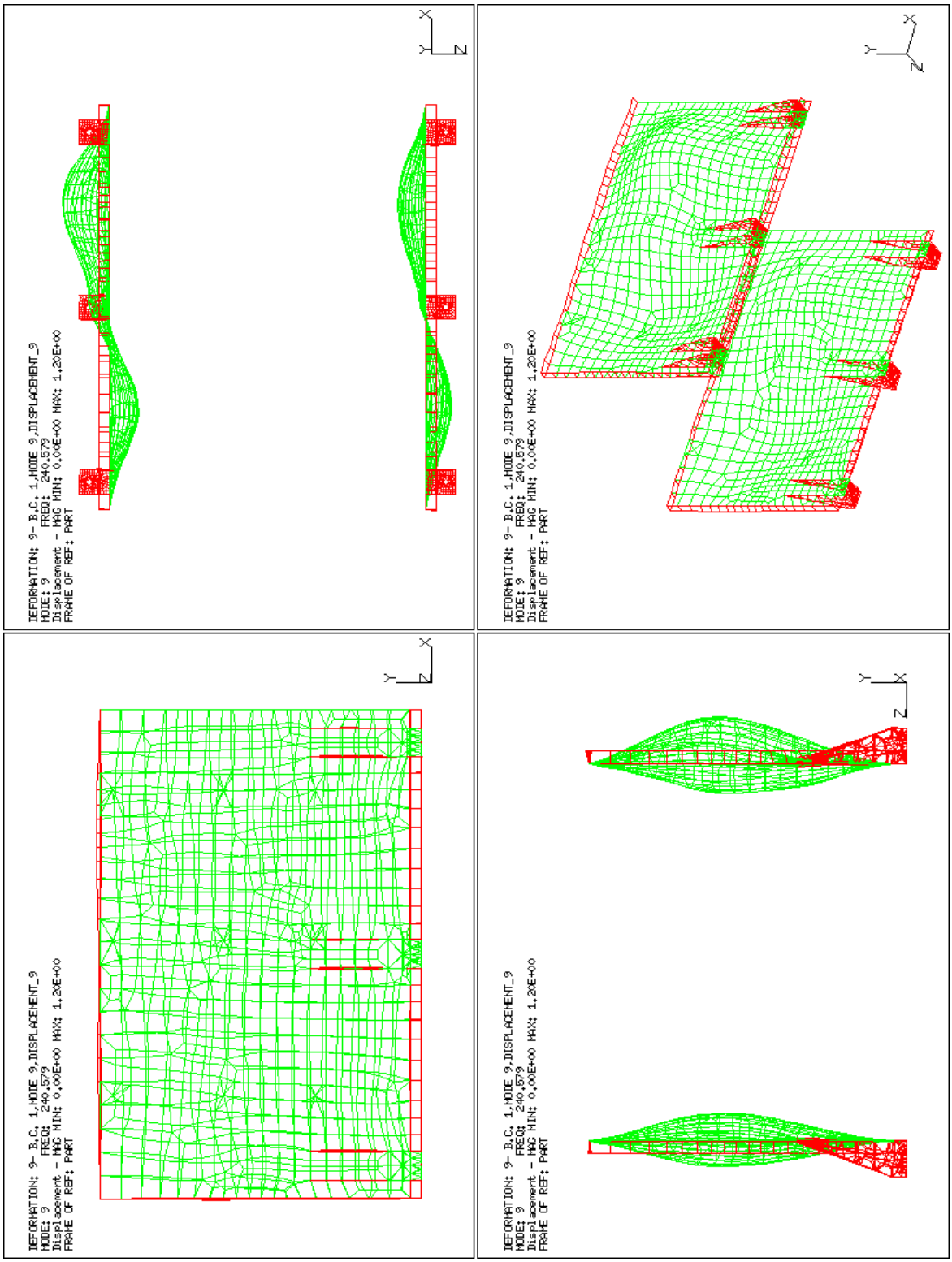
DEFORMATION: 9- B.C. 1,MODE 9,DISPLACEMENT_9
MODE: 9 FREQ: 240.579
Displacement - MAG MIN: 0.00E+00 MAX: 1.20E+00
FRAME OF REF: PART
DEFORMATION: 9- B.C. 1,MODE 9,DISPLACEMENT_9
MODE: 9 FREQ: 240.579
Displacement - MAG MIN: 0.00E+00 MAX: 1.20E+00
FRAME OF REF: PART
DEFORMATION: 9- B.C. 1,MODE 9,DISPLACEMENT_9
MODE: 9 FREQ: 240.579
Displacement - MAG MIN: 0.00E+00 MAX: 1.20E+00
FRAME OF REF: PART
DEFORMATION: 9- B.C. 1,MODE 9,DISPLACEMENT_9
MODE: 9 FREQ: 240.579
Displacement - MAG MIN: 0.00E+00 MAX: 1.20E+00
FRAME OF REF: PART

Mode 10

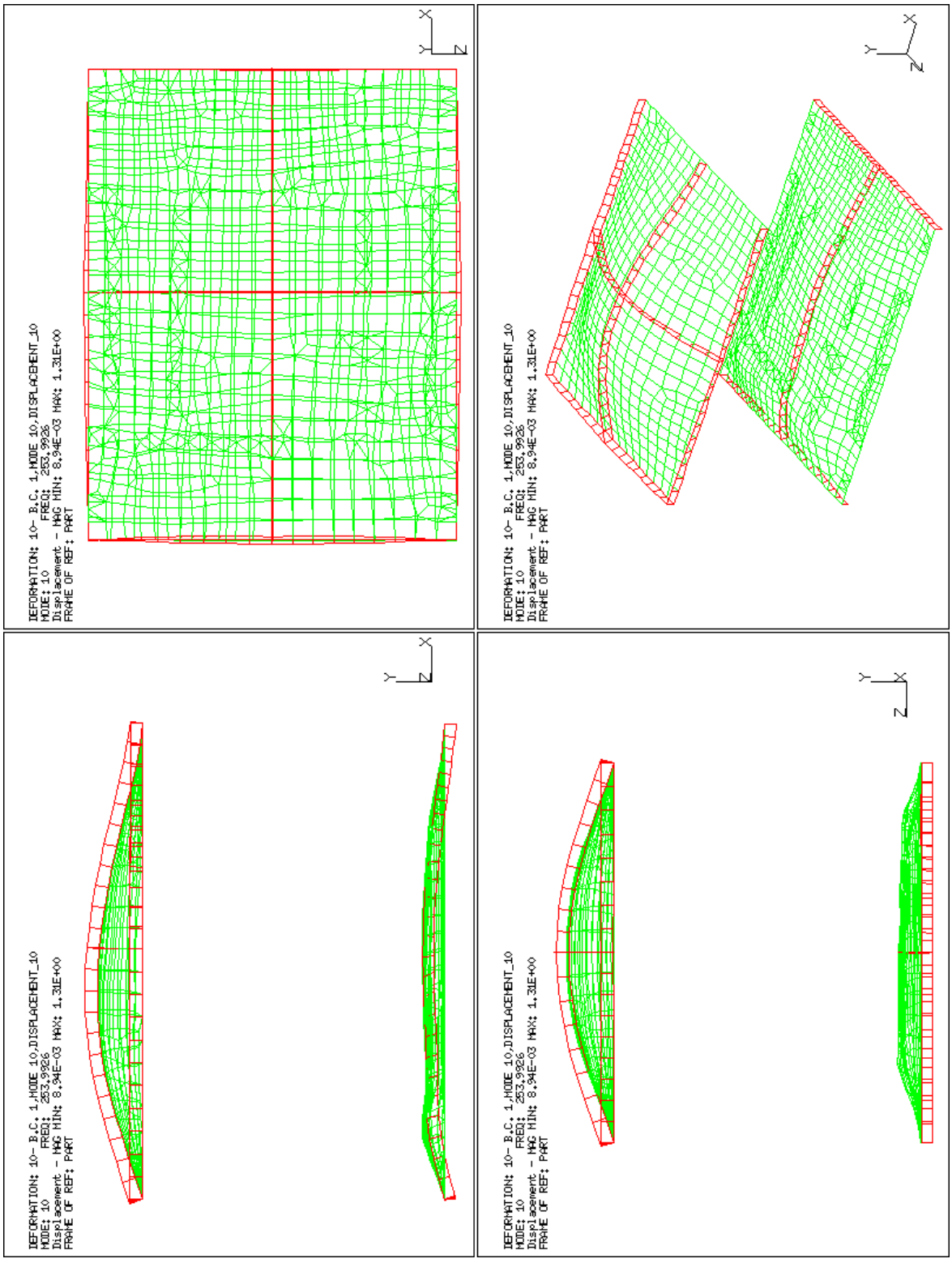
DEFORMATION: 10- B.C. 1,MODE 10,DISPLACEMENT_10
MODE: 10
FREQ: 253.9926
Displacement - MAG MIN: 8.94E-03 MAX: 1.31E+00
FRAME OF REF: PART